Interrogating the structure and function of the human voltage-gated proton channel (hH_v1) with a fluorescent noncanonical amino acid.

Emerson M. Carmona, William N. Zagotta*, Sharona E. Gordon*.

Department of Neurobiology and Biophysics, University of Washington, Seattle, WA, U.S.

*William N. Zagotta and Sharona E. Gordon.

Email: zagotta@uw.edu, seg@uw.edu

Author Contributions: All the authors conceived the study and designed the experiments. E.M.C. performed the experiments and analyzed the data. All the authors interpreted the data. E.M.C. wrote the first version of the manuscript. All the authors critically revised the article.

Competing Interest Statement: The authors declare no competing interests.

Abstract

The human voltage-gated proton channel (hH_v1) is a dimer of voltage-sensor domains (VSDs) containing highly selective proton permeation pathways in each monomer. In addition to voltage, hH_v1 is regulated by other stimuli, including pH gradients, mechanical forces, and ligands such as Zn^{2+}. Aside from the VSDs, this membrane protein contains an N-terminal domain and a C-terminal coiled-coil domain (CC) formed between the monomers. To address the need for direct measurements of conformational rearrangements in hH_v1, we developed a Förster resonance energy transfer (FRET) approach to measuring the conformational rearrangements in full-length hH_v1 purified from *E. coli*. We used genetic code expansion (GCE) to generate a library of 14 full-length hH_v1 constructs, each incorporating the fluorescent noncanonical amino acid acridon-2-ylalanine (Acd) at a different site throughout the various structural domains. Following the expression and purification of these hH_v1-Acd proteins, we found that 12 sites yielded stable and functional proton-permeable channels. The fluorescence properties of Acd at each site showed small site-specific differences. Furthermore, we measured site-specific FRET efficiencies from tryptophan (Trp) and tyrosine (Tyr) to Acd in the hH_v1-Acd proteins and found results consistent with correct folding in detergent micelles. Finally, the addition of Zn^{2+} produced reversible changes in FRET, with affected residues clustered on the intracellular side of the channel.

Introduction

The human voltage-gated proton channel (hH_v1) is a membrane protein that forms a proton selective channel (1, 2). Despite its physiological importance, its molecular mechanisms are still poorly understood, including the precise structural identity of the permeation pathway and the gating mechanism of voltage (3, 4), pH gradients (3, 5), membrane stretch (6), and ligands such as the classical inhibitor Zn^{2+} (7, 8). Understanding these processes requires connecting the functional properties to the hH_v1 structure.

Each monomer of hH_v1 dimers includes an intracellular N-terminal domain of unknown function, a transmembrane voltage-sensor domain (VSD), and an intracellular coiled-coil (CC), which forms the primary intersubunit interface (9, 10). Current structural models, however, have been obtained from truncated or chimeric channel constructs (11, 12), and thus, it is not clear whether they correspond to physiological or functional conformations. Moreover, the multiple kinetic components of H_v1 gating currents suggest that the protein's resting state comprises an ensemble of conformations (4, 5), which is consistent with the conformational flexibility inferred from structural approaches (12–14). Because protein function arises from this distribution of conformational states (15), approaches to directly measure structural heterogeneity in the full-length hH_v1 are needed.

An attractive approach to interrogate the structural heterogeneity of hH_v1 is fluorescence spectroscopy, which offers high sensitivity at nanomolar protein concentrations and compatibility with near-physiological conditions. Fluorescence can report on local environment and accessibility changes, as well as quantify distance changes through Förster resonance energy transfer (FRET) (16). Importantly, time-resolved FRET measured using lifetimes preserves information about conformational heterogeneity on the nanosecond timescale, which is lost in steady-state measurements due to the averaging process (17). Together, these capabilities make fluorescence, especially time-resolved FRET, a powerful method to connect hH_v1 structure and function (18).

A few obstacles remain to directly measuring conformational heterogeneity of hH_v1. First, a method to express and purify stable and functional protein is needed, which is challenging for membrane proteins. Second, site-specific fluorophore labeling is difficult at buried sites, resulting in low labeling efficiency. Third, traditional fluorophores are bulky and have long linkers (14), resulting in protein structure perturbation and heterogeneity dominated by the properties of the label (19). A recent method was optimized for robust expression and purification of full-length, functional hH_v1 in *E. coli* (20, 21). The remaining obstacles can be overcome by labeling the protein with the fluorescent noncanonical amino acid acridon-2-ylalanine (Acd) using genetic code expansion (GCE) (22–24). This technology allows site-specific labeling during translation by reassigning an amber stop codon using an orthogonal aminoacyl-tRNA synthetase (RS)/tRNA (25, 26) (Figure 1A). Acd's small size and minimal linker reduce perturbations and heterogeneity, and its favorable photophysics support both steady-state and time-resolved measurements (27). Here, we incorporated Acd across all hH_v1 structural domains and purified 12 of 14 constructs as stable, functional proteins. We then used Acd's environmental sensitivity and FRET from tryptophan (Trp)/tyrosine (Tyr) to Acd to validate the protein folding and report Zn^{2+}-dependent conformational changes. These data establish a platform for interrogating conformational heterogeneity and dynamics in the full-length hH_v1.

Results

We generated a library of hH_v1 constructs with Acd incorporated across the different structural domains. Because available H_v1 structural models were produced from either truncated or modified proteins (11, 12), we used an AlphaFold model of the full-length, dimeric hH_v1 to guide Acd site selection (28, 29) (Figure 1B and Dataset S1). The model recapitulates the expected hH_v1 architecture with high confidence: S0 as a short helix parallel to the membrane, S1-S4 transmembrane segments forming a canonical VSD, and a C-terminal helix extending from S4 that forms the CC intersubunit interface. In addition, two

99 helices in the N-terminal domain (P1 and P2) were predicted (Figure 1C), albeit
100 with low confidence. The dimer interface in the membrane is primarily formed by
101 S4-S4 contacts (Figure S1A), although S1-S1 contacts have been observed
102 experimentally (9, 13). This model appears to represent an intermediate state,
103 with the first S4 positive charged residue R208 proximal to D112 in the selectivity
104 filter, and the third S4 positive charged residue R211 proximal to F150 in the
105 charge-transfer center (Figure S1B). Although the model's accuracy and
106 functional state are unknown, we used it as a rough starting point for selecting
107 positions to incorporate Acd.

108 To test the feasibility and specificity of Acd incorporation in hH_v1, we
109 initially selected two positions in the intracellular domains: A18 in the N-terminal
110 domain and F247 in the CC. For each position, the wild-type codon was replaced
111 with an amber stop codon (TAG). Bacteria co-transformed with the Acd RS/tRNA
112 pair and hH_v1-TAG constructs expressed fluorescent full-length protein only
113 when Acd was present in the culture medium (Figure 1D). We next generated a
114 library of 14 constructs in which Acd was incorporated into every structural
115 domain: the N-terminal domain, each helix of the VSD, and the CC (Figure 2A-
116 B). Remarkably, most of the 14 hH_v1-Acd proteins expressed at levels
117 comparable to the control (No TAG) (Figure 2C and S2). As expected, several
118 hH_v1-Acd proteins also produced TAG-truncated products (Figure 2C).
119 Increasing the Acd concentration in the *E. coli* growth medium did not reduce the
120 fraction of truncated protein (Figure S3). One of the constructs, hH_v1-C107Acd,
121 showed a weak in-gel fluorescence signal, although the Western blot signal was
122 comparable to that of other constructs.
123

124 **We successfully purified stable and functional hH_v1 labeled with Acd at 12**
125 **of the 14 selected positions.** We attempted to purify all expressed hH_v1-Acd
126 constructs by immobilized metal affinity chromatography using the detergent
127 Anzergent 3-12 (20, 21). For 12 of 14 constructs, purification yielded a single
128 fluorescent band on SDS-PAGE (Figure 3A and S4). In contrast, no purified
129 protein was detected for the V187Acd or Q233Acd constructs (Figure S4).

130 Because hH_v1-Q233Acd was robustly expressed (Figure 2C), its loss during
131 purification suggests reduced stability. The hH_v1-Acd yields were construct-
132 dependent (Figure 3B), and the TAG-truncated products did not co-purify with the
133 full-length protein (Figure 3A and S4).
134 We then evaluated the stability and homogeneity of the hH_v1-Acd proteins
135 using fluorescence-detection size exclusion chromatography (FSEC) (30).
136 Similar to the control (Figure S5), most hH_v1-Acd proteins showed a predominant
137 main peak (~11.5 mL), which corresponds to the dimer (Figure S5), followed by a
138 minor peak at higher elution volumes (Figure 3C; Table S1). The proportion of
139 these two peaks varied between constructs (Figure S6). To determine whether
140 the purified hH_v1-Acd proteins were functional, we reconstituted the FSEC
141 fractions containing both peaks in asolectin liposomes and assessed their
142 function using a liposome proton flux assay (20, 31). All 12 reconstituted
143 constructs produced ACMA fluorescence quenching upon valinomycin addition,
144 indicating that our purified proteins formed functional proton-permeable channels
145 (Figure 3D and S7). These results highlight the versatility of GCE for
146 incorporating Acd as a fluorescent probe for structural studies of hH_v1.
147
148 **Acd was relatively insensitive to the hydrophobicity of its local**
149 **environment.** To explore how the local environment can alter Acd's spectral
150 properties, we measured the emission spectra of the free amino acid in different
151 solvents (Figure 4A and Table S2). The environmental sensitivity of Acd has
152 been studied previously (24, 27, 32), but we expanded this work here by using
153 the aprotic solvent ethyl acetate (EtAc) and a series of alcohols with varying alkyl
154 chain lengths. Consistent with a general solvent effect produced by polarity (16),
155 the emission spectrum was blue-shifted by approximately 20 nm in EtAc, the
156 least polar solvent measured, relative to water (Figure 4A and Table S2).
157 Alcohols produced a consistently smaller blue shift, independent of their alkyl-
158 chain length (Figure 4A). The spectrum in Buffer-H2, our standard experimental
159 solution containing detergent micelles, was only very slightly blue-shifted relative
160 to water (Figure 4A), suggesting that Acd did not substantially partition into the

161 hydrophobic core of the detergent micelles. We also tested whether solvent
162 polarity affects the fluorescence lifetime of Acd using time-correlated single
163 photon counting (TCSPC). The fluorescence lifetime of Acd showed a similar
164 trend to the spectral shifts (Figure 4B): EtAc shortened the lifetime markedly, Acd
165 exhibited shorter lifetimes in alcohols than in water, and Acd in Buffer-H2 had a
166 lifetime similar to that measured in water.

167 The spectral blue-shift and short lifetime of Acd in EtAc suggest that Acd
168 may be able to report on the local environment at different sites in hH_v1,
169 especially those that are surface-exposed versus those that face the lipid core.
170 The emission spectra of the hH_v1-Acd proteins showed small, site-specific shifts
171 (Figure 4C and Table S3). The local environment of Acd in hH_v1 spanned the
172 range between those observed for free Acd in Buffer-H2 and in alcohols, with
173 Q56Acd in the N-terminal intracellular domain and C107Acd in S1 showing the
174 most red-shifted and blue-shifted spectra, respectively (Figure 4C). Consistent
175 with the spectra, the fluorescence lifetimes of the hH_v1-Acd proteins fell between
176 those measured for free Acd in Buffer-H2 and in alcohols, with Q56Acd exhibiting
177 the slowest, and C107Acd the fastest, lifetimes (Figure 4D). While small, the
178 differences in spectral properties of Acd in hH_v1 agree with their predicted
179 location in the structural model, with C107 being the site closest to the detergent
180 micelles' hydrophobic core. The low sensitivity to polarity and pH changes (33) of
181 Acd in different hH_v1 local environments makes it well suited for measuring FRET
182 (27, 34).

183

184 **FRET between Trp/Tyr and Acd in hH_v1 suggested that the proteins are**
185 **properly folded.** Trp and Tyr have fluorescence emission spectra that overlap
186 with the Acd absorption spectrum and therefore can act as FRET donors to Acd,
187 with relatively short R_0 values (23.5 Å for Trp; 20.9 Å for Tyr) (22) (Figure 5A).
188 Each hH_v1 monomer contains four Trp and four Tyr residues (yellow spheres in
189 Figure 5B). In this structural model, the Trp residues are located in the N-terminal
190 domain (W4, W38, and W45) and midway along transmembrane segment S4 in
191 the VSD (W207). The Tyr residues are located in the N-terminal domain (Y35

192 and Y42) and near the extracellular end of transmembrane segment S2 (Y134
193 and Y141).

194 To quantify Trp/Tyr to Acd FRET, we used spectral FRET analysis (35).
195 The total emission spectrum from Trp/Tyr and Acd was collected (Figure 5C).
196 The Acd emission spectrum was extracted by subtracting a scaled Trp/Tyr
197 spectrum collected from control wild-type protein ($F_{280,NoTAG}$) (Figure 5D and S8).
198 For each Acd-containing construct, the ratio of the extracted spectrum (F_{280} –
199 $F_{280,NoTAG}$) to the Acd spectrum with direct excitation (F_{370}) was calculated as
200 *Ratio A* (Figure 5D and 5E). Because *Ratio A* is not wavelength-dependent, it
201 reports the linearity of the detectors and the absence of significant contamination
202 from other sources of fluorescence. The *Ratio A* component caused by the direct
203 excitation of Acd (termed *Ratio* A_0) was measured with free Acd (36) (Figure 5E
204 and S9). The difference between *Ratio A* and *Ratio* A_0 is directly proportional to
205 the FRET efficiency.

206 As expected, the *Ratio A* values for our hH_v1-Acd proteins were largely flat
207 across emission wavelengths for our hH_v1-Acd proteins (Figure 5E). For all Acd
208 sites, *Ratio A* was greater than *Ratio* A_0 (dashed line in Figure 5E), reflecting
209 FRET between Trp/Tyr and Acd at every site in hH_v1. Most *Ratio A* values were
210 distributed between 0.60 and 0.80, with two clear exceptions: A18Acd (blue) and
211 F247Acd (magenta) (Figure 5E). A18Acd showed the highest *Ratio A*, consistent
212 with the multiple Trp/Tyr residues in the N-terminal domain. Conversely,
213 F247Acd showed the lowest *Ratio A*, consistent with its location in the CC, far
214 from most Trp/Tyr residues (Figure 5B).

215 We next compared *Ratio A* – *Ratio* A_0 values with FRET efficiencies
216 predicted by the AlphaFold structural model. We modeled rotamer ensembles for
217 Trp, Tyr, and our Acd sites in the hH_v1 structural model using chiLife (37) and
218 calculated donor-acceptor distance distributions. These distributions were then
219 used to calculate FRET efficiencies (details in SI Text). The experimentally
220 determined *Ratio A* – *Ratio* A_0 values showed a moderate correlation (Pearson's
221 r = 0.48) with the calculated efficiencies (Figure 5F). Using the predicted
222 intrasubunit FRET efficiencies reduced the Pearson's r value to 0.18 (Figure

223 S10), suggesting that the measured FRET contains information about subunit
224 organization.
225 There were two spatially clustered deviations between experiment and
226 model. Positions at the extracellular ends of the VSD helices (Y134 in S2, K125
227 in S1, and F195 in S4) showed higher experimental FRET than predicted,
228 indicating shorter effective donor-acceptor distances relative to the model.
229 Conversely, positions on the intracellular side of the VSD (K169 in S3 and I217 in
230 S4) showed lower experimental FRET than predicted, implying longer effective
231 donor-acceptor distances. Together, the spatial clustering of residues with similar
232 deviations indicates specific deficits in the AlphaFold model or the failure to
233 quantify the protein dynamics.
234
235 **Zinc binding changed the conformation of hH$_v$1.** We next asked whether
236 FRET from Trp/Tyr to Acd could report conformational changes upon addition of
237 Zn^{2+}, the classical inhibitor of H$_v$1 proton currents in cells (7, 38, 39). The two
238 experimental structures of H$_v$1 were resolved with this cation bound to the
239 extracellular side of the VSD (11, 12). We observed site-specific spectral
240 changes in the hH$_v$1-Acd proteins in the presence of Zn^{2+} (Figure 6 and S11).
241 The largest changes occurred for hH$_v$1-K169Acd, where 1 mM Zn^{2+} caused a
242 decrease in the Trp/Tyr emission and an increase in the Acd emission (Figure
243 6A). This decrease in donor fluorescence, paired with increased acceptor
244 fluorescence, is the hallmark of increased FRET and was corroborated by
245 spectral analysis (Figure 6B). Additionally, a slight blue shift of the Trp/Tyr
246 fluorescence was observed for all hH$_v$1-Acd proteins in the presence of Zn^{2+}
247 (Figure S11). These changes were completely reversed by the addition of EDTA,
248 confirming that the changes arise from a reversible conformational change upon
249 Zn^{2+} binding (Figure 6A and 6B). Large changes in effective FRET efficiency
250 were observed with Acd incorporated at Q56 in the N-terminal domain and C107,
251 F159, and K169 in the VSD (Figure 6C). Notably, these positions are
252 intracellular, even though H$_v$1 currents are inhibited by extracellular Zn^{2+} (7, 40).
253 These results are consistent with previous studies showing that some

254 extracellular H_v1 inhibitors, such as Zn^{2+} or AGAP, induce long-range structural
255 changes that propagate to the channel's intracellular vestibule (41, 42) and
256 persist in detergent micelles (12).
257
258
259 **Discussion**
260 Incorporating Acd into hH_v1 by GCE opens new possibilities for studying
261 the structure and function of this channel. We systematically incorporated Acd at
262 multiple positions in hH_v1 and confirmed protein stability and function after
263 purification. 12 of 14 hH_v1-Acd proteins produced acceptable yields upon
264 purification and were functional, despite being a human membrane protein
265 expressed in *E. coli*. Two factors likely underlie the robustness of our system: (i)
266 an optimized purification protocol for hH_v1 (20, 21) that offsets the expected
267 reduction in yield associated with GCE (22, 25), and (ii) the high efficiency and
268 specificity of the evolved aminoacyl-tRNA synthetase for incorporating Acd (17,
269 27).
270 Fluorescence spectroscopy has been used to detect conformational
271 changes in H_v1. Sites at the extracellular portion of S4 (43) and S1 (44) in the
272 VSD of *Ciona intestinalis* H_v1 have been labeled with the fluorophores Alexa488
273 and tetramethylrhodamine (TAMRA) through cysteine-selective reagents to
274 capture conformational changes during activation using voltage-clamp
275 fluorometry. Similarly, the fluorescent noncanonical amino acid 3-(6-
276 acetylnaphthalen-2-ylamino)-2-aminopropanoic acid (Anap) has been
277 incorporated at several sites in the S4 in hH_v1 (45) to study conformational
278 changes in response to voltage and pH. In these cases, the fluorophore's
279 environmental sensitivity has been used as a readout of conformational changes.
280 By contrast, FRET provides richer structural information due to its distance
281 dependence. Single-molecule FRET has been measured in purified hH_v1 labeled
282 with Cy3 and Cy5 to track the VSD movements in response to voltage, pH,
283 cholesterol, and zinc (14, 46). The small size and minimal linker of Acd, along

284 with its low environmental sensitivity and high photostability, are advantageous
285 for measuring FRET in hH_v1 compared with previously used fluorophores.
286 The high number of FRET donors, 4 tryptophans and 4 tyrosines per
287 subunit, limits the utility of the Trp/Tyr-Acd FRET pair as a strategy to measure
288 conformational rearrangements in hH_v1. Our library of a dozen single Acd-
289 incorporating constructs, with sites distributed across the entire primary
290 sequence of the protein, opens the door to using Acd as a FRET donor. We have
291 previously used time-resolved transition metal ion FRET (tmFRET), which utilizes
292 a transition metal ion as a FRET acceptor (27, 34), to measure conformational
293 energetics in the bacterial cyclic nucleotide-gated ion channel SthK (47).
294 However, in that work, we incorporated Acd at a single position in the intracellular
295 C-terminal domain of SthK. With Acd incorporated at multiple sites in full-length
296 hH_v1, it will be possible to interrogate conformational changes across the
297 protein's different structural domains using Acd as a tmFRET donor to
298 understand its molecular mechanisms.
299
300
301 **Materials and Methods**
302 **Protein expression and purification.** hH_v1 was expressed and purified
303 according to the published protocol with minor modifications (20, 21). Briefly,
304 fresh competent BL21-Gold(DE3) cells (Agilent) were co-transformed with the
305 His-EK-hH_v1-C107A-C249A.pET15-b (hH_v1-Cysless, referred to as No TAG) and
306 MjA9Acd-RS.pDule2 (22, 23) plasmids (sequences in SI Text) using the heat
307 shock method. For expressing hH_v1-Acd proteins, the codon corresponding to
308 the selected position was changed to the amber stop codon (TAG) by site-
309 directed mutagenesis. All plasmids were sequenced before use. Pre-cultures
310 were grown overnight in LB medium supplemented with 0.2% glucose, 0.4
311 mg/mL ampicillin, and 0.1 mg/mL spectinomycin at 37 °C and 250 rpm. The next
312 day, cultures were diluted 1:100 in complete autoinduction medium (48)
313 supplemented with 0.4 mg/mL ampicillin and 0.1 mg/mL spectinomycin, and then
314 grown at 37 °C and 250 rpm until an OD_{600} of 1.5 was reached. The protein

315 expression level was proportional to the Acd concentration in the culture medium
316 (Figure S12). We chose 0.6 mM Acd in the culture medium as optimal for hH_v1
317 expression, as higher concentrations only slightly increased the final biomass
318 (Figure S12B). Cultures supplemented with 0.6 mM Acd were grown overnight at
319 20 °C and 250 rpm. Cells were then harvested, resuspended in Buffer-H1 (50
320 mM Tris, 150 mM NaCl, 1 mM benzamidine, 0.17 mg/mL PMSF, pH 8.0)
321 supplemented with 0.5 mg/mL lysozyme, and incubated for 30 min at 4 °C before
322 being flash-frozen. After thawing, the extracts were supplemented with 5 mM
323 $MgCl_2$, fresh protease inhibitors, and 12.5 μg/mL DNase I, incubated for 1 h at 4
324 °C, sonicated, and centrifuged at 100,000g at 4 °C for 1 h. The membrane pellet
325 was resuspended in Buffer-H1 and stored at -80 °C until further use. After
326 thawing, the membranes were solubilized with 1.5% Anzergent 3-12 (Anatrace)
327 (Anz3-12) at room temperature for 1 hour. Insoluble material was removed by
328 centrifuging at 100,000g and 4 °C for 1 h, and the solubilized membrane extract
329 was incubated with His-Pur Ni-NTA (Thermo Scientific) resin equilibrated with
330 Buffer-H2 (50 mM Tris, 150 mM NaCl, 12 mM Anz3-12, pH 8.0) for 1 hour at
331 room temperature. Resin was collected in a gravity column and washed with 20
332 column volumes (CV) of Buffer-H2, followed by 16 CV of Buffer-H2 with 90 mM
333 imidazole. The hH_v1 protein was eluted with 20 CV of Buffer-H2 with 0.5 M
334 imidazole, was concentrated with 50kDa cut-off centrifugal filters, and imidazole
335 was removed by FSEC (Ex/Em = 385/450 nm) in an ENrich SEC 650 (Bio-Rad)
336 column with Buffer-H2. The hH_v1-containing fractions were concentrated to 0.5-
337 1.5 mg/mL, depending on the amount of purified protein, and then aliquoted,
338 flash-frozen, and stored at -80 °C until use.
339
340 **Reconstitution and fluorescence proton flux assays.** The hH_v1-Acd samples
341 were reconstituted and assayed using a liposome proton flux assay, as described
342 previously, with minor modifications (20). Briefly, soy polar lipid extract (Avati) in
343 chloroform was dried overnight at room temperature in a rotary evaporator under
344 vacuum and then hydrated in Buffer-K (20 mM HEPES, 150 mM KCl, and 1 mM
345 EDTA, pH 7.0) to a concentration of 10 mg/mL. The vesicles were sonicated in a

346 water bath until the solution became translucent, aliquoted, flash-frozen, and
347 stored at -80 °C until further use. Reconstitutions were performed at a 1:100
348 (protein:lipid, by mass) ratio by mixing 12.5 μg of purified hH_v1-Acd with 1.25 mg
349 of liposomes in a final volume of 330 μL Buffer-K containing 8 mM Anz3-12. The
350 mixture was incubated at room temperature for 1 h, then diluted with 5 mL of
351 Buffer-K and incubated for 30 min. The mixture was further incubated with three
352 cumulative pulses of 100 mg Bio-Beads SM2 (Bio-Rad), each for 1 h at room
353 temperature. After the final Bio-Beads pulse, the mixture was incubated overnight
354 at 4 °C. The next day, two successive 100 mg additions of Bio-Beads were
355 performed, with a 1-hour incubation at room temperature following each addition.
356 Bio-Beads were removed in a gravity column, the mixture was diluted with 10 mL
357 of Buffer-K, and then centrifuged at 150,000g for 2 hours at 4 °C. The
358 proteoliposome pellets were resuspended in 250 μL of Buffer-K, aliquoted, flash-
359 frozen, and stored at -80 °C until further use. On the day of the liposome proton
360 flux assays, samples were thawed at 37 °C and then placed on ice. The sample
361 (40 μL) was diluted in Buffer-Na (20 mM HEPES, 150 mM NaCl, 1 mM EDTA, pH
362 7.0). 9-Amino-6-chloro-2-methoxyacridine (ACMA; Sigma) was added to a final
363 concentration of 2 μM from a 2 mM stock solution in DMSO, and the mixture was
364 incubated at room temperature for 5 minutes before the fluorescence
365 measurement began. The baseline was recorded for 3 min (F_{max}). Subsequently,
366 10 nM of valinomycin (Cell Signaling) was added from a 10 μM stock solution in
367 DMSO, followed by 1 μM carbonyl cyanide m-chlorophenyl hydrazone (CCCP;
368 Sigma) from a 1 mM stock solution in DMSO to record F_{min}. The final volume was
369 2 mL. The fluorescence signal ($F(t)$) was normalized according to the equation
370 $(F(t)-F_{min})/(F_{max}-F_{min})$. Fluorescence measurements were performed at 5-second
371 intervals with a 2-second integration time using a Fluorolog-3 spectrometer
372 (Horiba) configured to an excitation wavelength of 410 nm (5 nm bandpass) and
373 an emission wavelength of 490 nm (1 nm bandpass) at room temperature.
374
375 **Absorption and fluorescence spectra recordings.** The absorption and
376 fluorescence spectra were recorded in the indicated solvents or fresh Buffer-H2

377 at room temperature. Absorption spectra were recorded in a DU 800
378 Spectrometer (Beckman Coulter) with a wavelength interval of 0.5 nm and a scan
379 speed of 600 nm/min. Fluorescence emission spectra were measured using a
380 Fluorolog-3 spectrometer (Horiba) with an integration time of 0.1 s, 1 nm
381 increments, and excitation and emission slits of 5 nm. For solubilizing Acd in
382 different solvents, a saturated solution of the amino acid was prepared by
383 dissolving 0.5 mg of Acd powder in the respective solvent. Acd spectra were
384 corrected by subtracting a blank of the solvent. hH_v1-Acd proteins were
385 measured at concentrations ranging from 180 to 240 nM in Buffer-H2. Each
386 spectrum was corrected by subtracting a blank with the solvent or Buffer-H2
387 before adding the protein sample to the cuvette.
388
389 **Spectral FRET analysis.** We used our previously established spectral FRET
390 analysis to remove contamination caused by direct excitation of Acd by 280 nm
391 light (36). This method had the added benefit of eliminating errors arising from
392 the recording system's transfer function, variations in the acceptor's quantum
393 yield, or variations in the total concentration of fluorescent molecules. A Trp/Tyr
394 spectrum was collected from control protein without any TAG codons (no Acd
395 incorporation). This was used to subtract the Trp/Tyr emission spectra collected
396 at 280 nm for each Acd-incorporating protein. This yielded the extracted Acd
397 spectrum, F_{280}, that had two components: the component due to direct excitation
398 of Acd, F_{280}^{direct}, and the component due to FRET, F_{280}^{FRET}. F_{280} was normalized by
399 the total Acd emission with 370 nm excitation, F_{370}. The resulting ratio, termed
400 *Ratio A*, can be expressed as: $Ratio\ A = \frac{F_{280}}{F_{370}} = \frac{F_{280}^{direct}}{F_{370}} + \frac{F_{280}^{FRET}}{F_{370}}$. The direct
401 excitation component, $\frac{F_{280}^{direct}}{F_{370}}$, termed *Ratio* A_0, was measured using free Acd
402 amino acid in Buffer-H2. We then quantified the relative FRET efficiency as
403 $Ratio\ A - Ratio\ A_0 = \frac{F_{280}^{FRET}}{F_{370}}$. This quantity is directly proportional to FRET
404 efficiency. An average *Ratio A* value was calculated between 410 and 480 nm.
405

406 **Time-resolved fluorescence measurements.** TCSPC measurements were
407 performed in a FluoTime 300 spectrometer equipped with a PMA Hybrid 40
408 detector and LDH-P-C-375 laser diode head (PicoQuant) at room temperature.
409 Emitted photons were detected at 446 nm with the emission polarizer at the
410 magic angle. The TCSPC measurements were performed in the indicated solvent
411 or fresh Buffer-H2. The hH_v1-Acd samples were measured at a concentration of
412 1 μM and the Acd amino acid at 500 nM. The count rate was always less than
413 1% of the excitation repetition rate to avoid pile-up distortions of the fluorescence
414 decay. The IRF was measured using a dilute Ludox solution in water.
415
416
417 **Acknowledgments**
418 We thank the Oregon State University GCE4ALL (Center for Genetic Code
419 Expansion for All) for their long-standing collaboration. We also appreciate the
420 excellent technical support provided by Dr. James Petersson and Kyle D. Shaffer
421 (University of Pennsylvania) with the Acd synthesis. This work was supported by
422 the National Institutes of Health under award numbers R01EY037223 and
423 R35GM145225 to S.E.G., and R01EY010329 and R35GM148137 to W.N.Z.
424 E.M.C. is a Pew Latin American Fellow.
425
426
427 **References**

428 1. M. Sasaki, M. Takagi, Y. Okamura, A Voltage Sensor-Domain Protein Is a Voltage-
429 Gated Proton Channel. *Science* **312**, 589–592 (2006).

430 2. I. S. Ramsey, M. M. Moran, J. A. Chong, D. E. Clapham, A voltage-gated proton-
431 selective channel lacking the pore domain. *Nature* **440**, 1213–1216 (2006).

432 3. V. V. Cherny, V. S. Markin, T. E. DeCoursey, The voltage-activated hydrogen ion
433 conductance in rat alveolar epithelial cells is determined by the pH gradient. *The*
434 *Journal of General Physiology* **105**, 861–896 (1995).

435 4. E. M. Carmona, *et al.*, Gating charge displacement in a monomeric voltage-gated
436 proton (H_v1) channel. *Proc. Natl. Acad. Sci. U.S.A.* **115**, 9240–9245 (2018).

437 5. E. M. Carmona, *et al.*, The voltage sensor is responsible for ΔpH dependence in H_v1
438 channels. *Proc. Natl. Acad. Sci. U.S.A.* **118**, e2025556118 (2021).

439 6. M. M. Pathak, *et al.*, The Hv1 proton channel responds to mechanical stimuli.
440 *Journal of General Physiology* **148**, 405–418 (2016).

441 7. V. V. Cherny, T. E. DeCoursey, pH-Dependent Inhibition of Voltage-Gated H^+
442 Currents in Rat Alveolar Epithelial Cells by Zn^{2+} and Other Divalent Cations. *The*
443 *Journal of General Physiology* **114**, 819–838 (1999).

444 8. T. E. DeCoursey, V. V. Cherny, Voltage-activated hydrogen ion currents. *J.*
445 *Membarin Biol.* **141** (1994).

446 9. S.-Y. Lee, J. A. Letts, R. MacKinnon, Dimeric subunit stoichiometry of the human
447 voltage-dependent proton channel H_v1. *Proc. Natl. Acad. Sci. U.S.A.* **105**, 7692–
448 7695 (2008).

449 10. H. P. Koch, *et al.*, Multimeric nature of voltage-gated proton channels. *Proc. Natl.*
450 *Acad. Sci. U.S.A.* **105**, 9111–9116 (2008).

451 11. K. Takeshita, *et al.*, X-ray crystal structure of voltage-gated proton channel. *Nat*
452 *Struct Mol Biol* **21**, 352–357 (2014).

453 12. M. Bayrhuber, *et al.*, Nuclear Magnetic Resonance Solution Structure and
454 Functional Behavior of the Human Proton Channel. *Biochemistry* **58**, 4017–4027
455 (2019).

456 13. Q. Li, *et al.*, Resting state of the human proton channel dimer in a lipid bilayer.
457 *Proc. Natl. Acad. Sci. U.S.A.* **112** (2015).

458 14. S. Han, *et al.*, Structural dynamics determine voltage and pH gating in human
459 voltage-gated proton channel. *eLife* **11**, e73093 (2022).

460 15. K. Henzler-Wildman, D. Kern, Dynamic personalities of proteins. *Nature* **450**, 964–
461 972 (2007).

462 16. J. R. Lakowicz, Ed., *Principles of Fluorescence Spectroscopy* (Springer US, 2006).

463 17. S. E. Gordon, M. Munari, W. N. Zagotta, Visualizing conformational dynamics of
464 proteins in solution and at the cell membrane. *eLife* **7**, e37248 (2018).

465 18. W. N. Zagotta, *et al.*, Measuring conformational equilibria in allosteric proteins
466 with time-resolved tmFRET. *Biophysical Journal* **123**, 2050–2062 (2024).

467 19. J. W. Taraska, M. C. Puljung, W. N. Zagotta, Short-distance probes for protein
468 backbone structure based on energy transfer between bimane and transition metal
469 ions. *Proc. Natl. Acad. Sci. U.S.A.* **106**, 16227–16232 (2009).

470 20. E. M. Carmona, D. M. Cortes, L. G. Cuello, A novel method for expressing and
471 purifying large quantities of functional and stable human voltage-gated proton
472 channel (hH_v1). *Protein Science* **34**, e70017 (2025).

473 21. E. Carmona, M. Cortes, L. Cuello, Expression and Purification of the Human
474 Voltage-Gated Proton Channel (hH_v1). *BIO-PROTOCOL* **15** (2025).

475 22. L. C. Speight, *et al.*, Efficient Synthesis and In Vivo Incorporation of Acridon-2-
476 ylalanine, a Fluorescent Amino Acid for Lifetime and Förster Resonance Energy
477 Transfer/Luminescence Resonance Energy Transfer Studies. *J. Am. Chem. Soc.* **135**,
478 18806–18814 (2013).

479 23. I. Sungwienwong, *et al.*, Improving target amino acid selectivity in a permissive
480 aminoacyl tRNA synthetase through counter-selection. *Org. Biomol. Chem.* **15**,
481 3603–3610 (2017).

482 24. C. M. Jones, *et al.*, Genetic encoding of a highly photostable, long lifetime
483 fluorescent amino acid for imaging in mammalian cells. *Chem. Sci.* **12**, 11955–
484 11964 (2021).

485 25. C. C. Liu, P. G. Schultz, Adding New Chemistries to the Genetic Code. *Annu. Rev.*
486 *Biochem.* **79**, 413–444 (2010).

487 26. T. S. Young, I. Ahmad, J. A. Yin, P. G. Schultz, An Enhanced System for Unnatural
488 Amino Acid Mutagenesis in E. coli. *Journal of Molecular Biology* **395**, 361–374
489 (2010).

490 27. W. N. Zagotta, *et al.*, An improved fluorescent noncanonical amino acid for
491 measuring conformational distributions using time-resolved transition metal ion
492 FRET. *eLife* **10**, e70236 (2021).

493 28. J. Jumper, *et al.*, Highly accurate protein structure prediction with AlphaFold.
494 *Nature* **596**, 583–589 (2021).

495 29. G. Kim, *et al.*, Easy and accurate protein structure prediction using ColabFold. *Nat*
496 *Protoc* **20**, 620–642 (2025).

497 30. T. Kawate, E. Gouaux, Fluorescence-Detection Size-Exclusion Chromatography for
498 Precrystallization Screening of Integral Membrane Proteins. *Structure* **14**, 673–681
499 (2006).

500 31. S.-Y. Lee, J. A. Letts, R. MacKinnon, Functional Reconstitution of Purified Human
501 H_v1 H^+ Channels. *Journal of Molecular Biology* **387**, 1055–1060 (2009).

502 32. A. Szymańska, K. Wegner, L. Łankiewicz, Synthesis of *N*-[(*tert*-Butoxy)carbonyl]-3-
503 (9,10-dihydro-9-oxoacridin-2-yl)-L-alanine, a New Fluorescent Amino Acid
504 Derivative. *Helvetica Chimica Acta* **86**, 3326–3331 (2003).

505 33. S. G. Schulman, R. J. Sturgeon, Variations of fluorescence efficiencies of 9-(10H)-
506 acridone and its 4-methoxy derivative with pH. Excited-state proton transfer in
507 very weak acids and. *Analytica Chimica Acta* **93**, 239–247 (1977).

508 34. S. E. Gordon, *et al.*, Long-distance tmFRET using bipyridyl- and phenanthroline-
509 based ligands. *Biophysical Journal* **123**, 2063–2075 (2024).

510 35. R. M. Clegg, "[18] Fluorescence resonance energy transfer and nucleic acids" in
511 *Methods in Enzymology*, (Elsevier, 1992), pp. 353–388.

512 36. J. Zheng, M. D. Varnum, W. N. Zagotta, Disruption of an Intersubunit Interaction
513 Underlies Ca^{2+}-Calmodulin Modulation of Cyclic Nucleotide-Gated Channels. *J.*
514 *Neurosci.* **23**, 8167–8175 (2003).

515 37. M. H. Tessmer, S. Stoll, chiLife: An open-source Python package for in silico spin
516 labeling and integrative protein modeling. *PLoS Comput Biol* **19**, e1010834 (2023).

517 38. B. Musset, *et al.*, Zinc inhibition of monomeric and dimeric proton channels
518 suggests cooperative gating. *The Journal of Physiology* **588**, 1435–1449 (2010).

519 39. C. Jardin, G. Chaves, B. Musset, Assessing Structural Determinants of Zn^{2+} Binding
520 to Human H_v1 via Multiple MD Simulations. *Biophysical Journal* **118**, 1221–1233
521 (2020).

522 40. F. Qiu, *et al.*, Molecular mechanism of Zn^{2+} inhibition of a voltage-gated proton
523 channel. *Proc. Natl. Acad. Sci. U.S.A.* **113** (2016).

524 41. D. Tang, *et al.*, Scorpion toxin inhibits the voltage-gated proton channel using a
525 Zn^{2+}-like long-range conformational coupling mechanism. *British J Pharmacology*
526 **177**, 2351–2364 (2020).

527 42. V. De La Rosa, A. L. Bennett, I. S. Ramsey, Coupling between an electrostatic
528 network and the Zn^{2+} binding site modulates H_v1 activation. *Journal of General*
529 *Physiology* **150**, 863–881 (2018).

530 43. C. Gonzalez, H. P. Koch, B. M. Drum, H. P. Larsson, Strong cooperativity between
531 subunits in voltage-gated proton channels. *Nat Struct Mol Biol* **17**, 51–56 (2010).

44. L. Mony, T. K. Berger, E. Y. Isacoff, A specialized molecular motion opens the Hv1 voltage-gated proton channel. *Nat Struct Mol Biol* **22**, 283–290 (2015).

45. E. Suárez-Delgado, M. Orozco-Contreras, G. E. Rangel-Yescas, L. D. Islas, Activation-pathway transitions in human voltage-gated proton channels revealed by a non-canonical fluorescent amino acid. *eLife* **12**, e85836 (2023).

46. S. Han, *et al.*, Cholesterol inhibits human voltage-gated proton channel hHv1. *Proc. Natl. Acad. Sci. U.S.A.* **119**, e2205420119 (2022).

47. P. Eggan, S. E. Gordon, W. N. Zagotta, Domain Coupling in Allosteric Regulation of SthK Measured Using Time-Resolved Transition Metal Ion FRET. [Preprint] (2025). Available at: https://elifesciences.org/reviewed-preprints/106892v2 [Accessed 2 August 2025].

48. F. W. Studier, Protein production by auto-induction in high-density shaking cultures. *Protein Expression and Purification* **41**, 207–234 (2005).

Figures and Tables

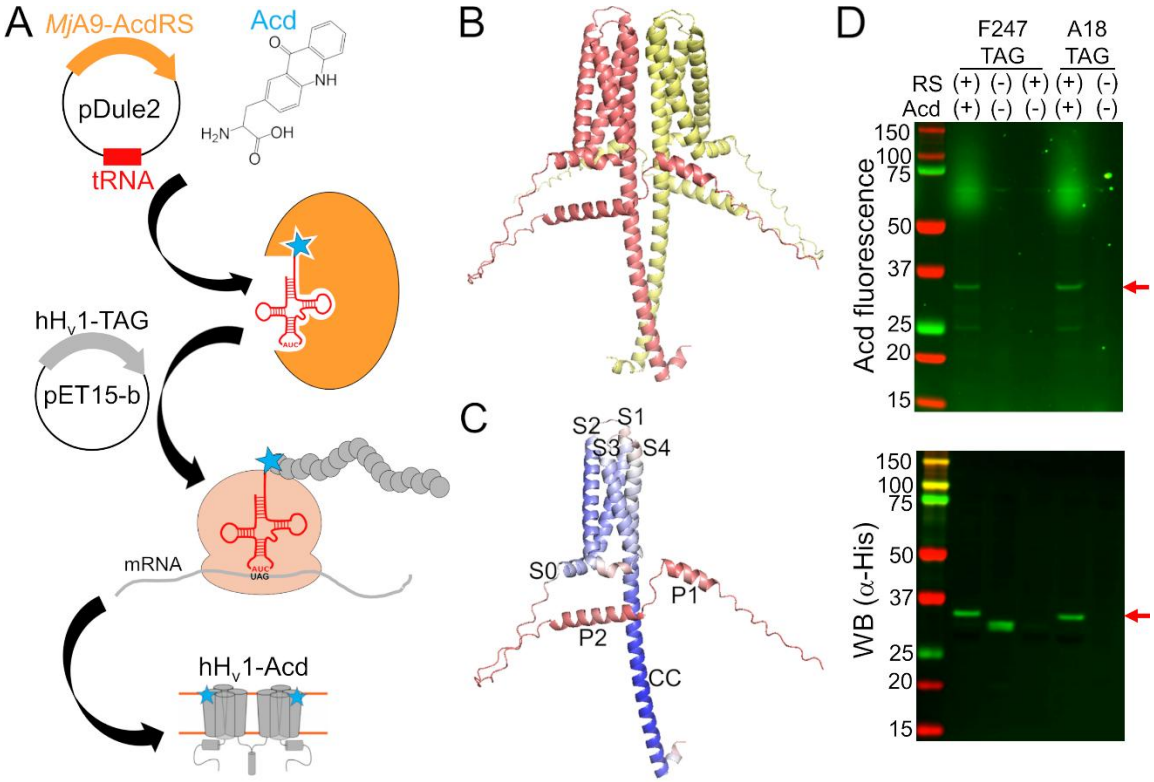

Figure 1. hHv1 was labeled with the fluorescent noncanonical amino acid Acd by genetic code expansion. (A) Cartoon showing the components of the

552 genetic code expansion system used to incorporate Acd via amber codon
553 suppression in hH_v1. (B) AlphaFold structural model of the dimer hH_v1 colored by
554 subunit. (C) AlphaFold structural model of a single hH_v1 subunit colored by the
555 predicted Local Distance Difference Test (pLDDT). Model confidence was
556 represented by a gradient from red to blue, indicating low to high pLDDT. (D) In-
557 gel fluorescence and Western blot to evaluate Acd incorporation. An Acd
558 fluorescence band corresponding to the molecular weight of full-length hH_v1 (red
559 arrow) was observed in cellular extracts after separation by SDS-PAGE only
560 when cells contained the *Mj*A9-AcdRS/tRNA plasmid (RS) and were grown in the
561 presence of 1mM Acd (top). The Western blot against the His-tag present at the
562 N-terminus of hH_v1 confirmed that the band corresponded to the recombinant
563 protein (bottom). Note the hH_v1 truncated product produced when the amber stop
564 codon is replacing F247 in the absence of the aminoacyl-tRNA synthetase/tRNA
565 plasmid and Acd.
566

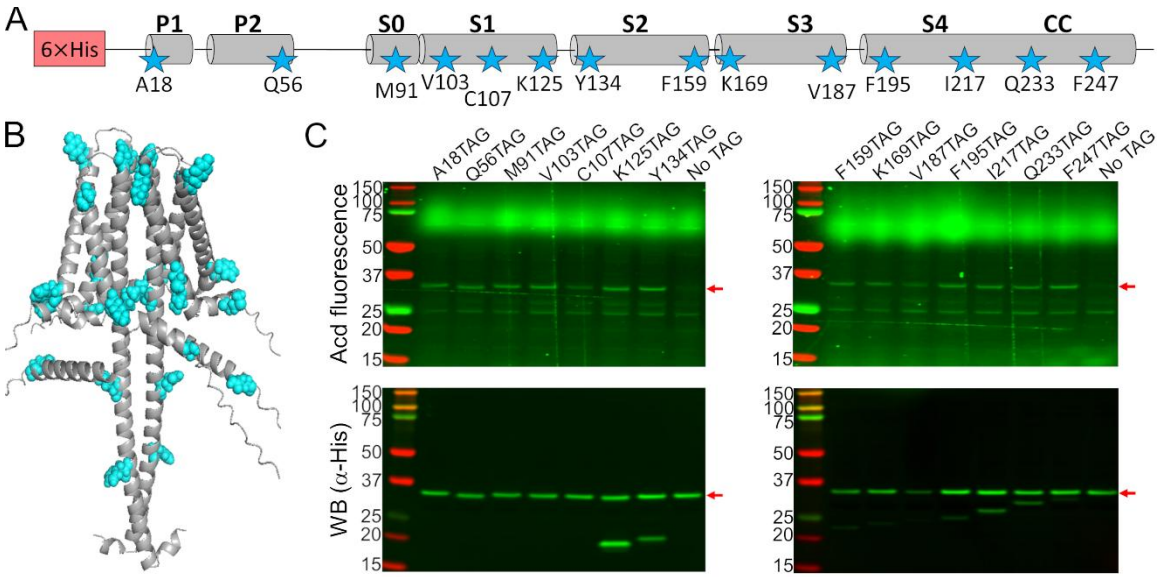

Figure 2. Acd was incorporated into 14 positions in the hH$_v$1 sequence. (A) Cartoon showing the amino acids selected to be replaced by an amber stop codon in the hH$_v$1 secondary structure to incorporate Acd (stars). (B) AlphaFold dimer hH$_v$1 structural model with the amino acids selected to be replaced by Acd as cyan spheres. (C) Acd fluorescence gel (top) and Western blot (bottom) of cellular extracts after separation by SDS-PAGE showing the expression of the Acd-labeled hH$_v$1 mutants (red arrows). The shorter detected bands in the WB for some constructs are produced by translation termination. The No TAG lane contains an extract from cells grown under identical conditions (in the presence of Acd and the aminoacyl-tRNA synthetase/tRNA pair) and expressing hH$_v$1 without an amber stop codon.

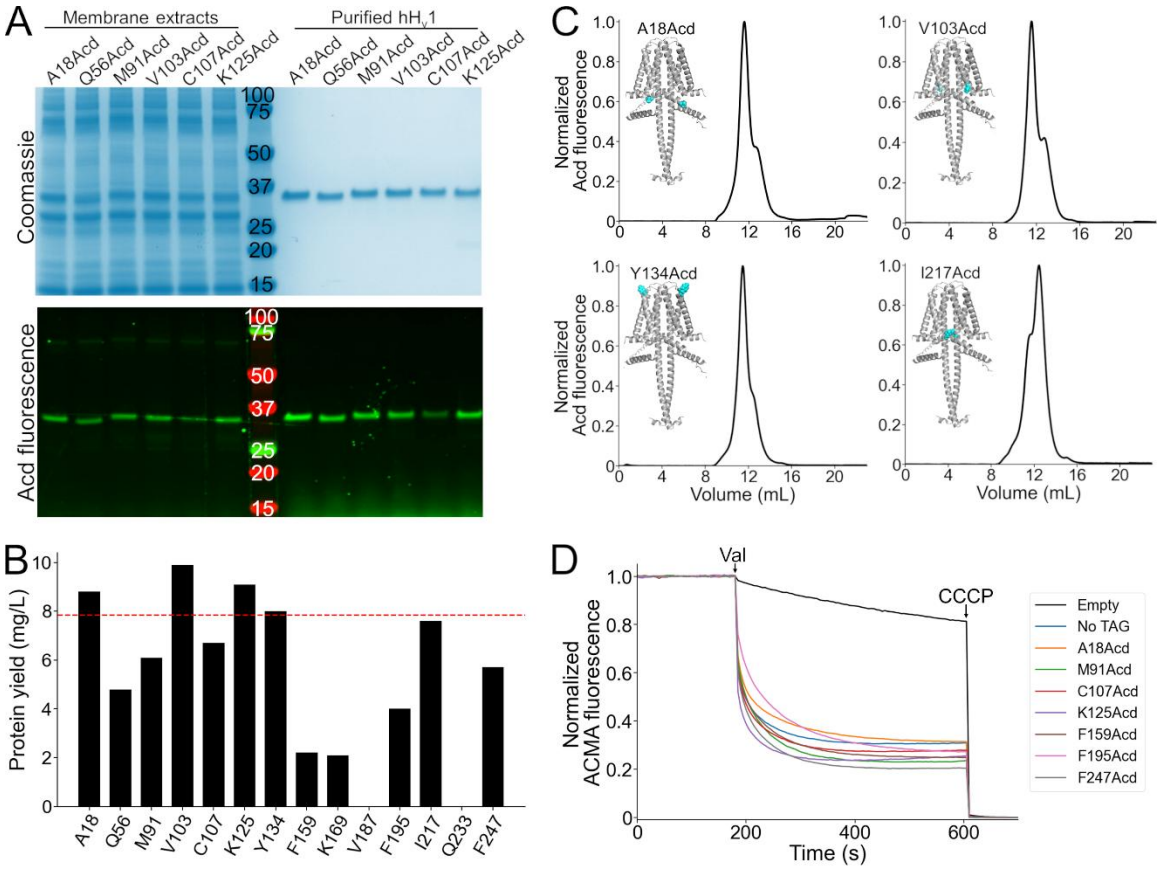

Figure 3. Purification and functional measurements of hHv1-Acd proteins. (A) Coomassie-stained (top) and Acd fluorescence (bottom) gels after separation by SDS-PAGE showing representative samples of the membrane extracts after solubilization (left) and the final purified protein after immobilized metal affinity chromatography (right). (B) Protein yield of the hHv1 protein with Acd replacing the amino acid at the indicated position. Note that V187Acd and Q233Acd contained no detectable protein after purification. The red line indicates the protein yield obtained from hHv1 without an amber stop codon in the presence of Acd and the aminoacyl-tRNA synthetase/tRNA pair (No TAG). (C) Representative fluorescence-detection size-exclusion chromatograms of the purified hHv1 proteins with Acd incorporated at the indicated amino acid position. Insets: AlphaFold dimer models, with the amino acid replaced by Acd shown as cyan spheres. (D) Representative liposome proton flux assay of asolectin proteoliposomes containing the indicated hHv1 protein. All purified proteins produced ACMA fluorescence quenching after the addition of valinomycin (Val). The protonophore CCCP was added at the end of the experiment as a control.

597 The No TAG sample corresponds to proteoliposomes containing hH_v1 without an
598 amber stop codon expressed in the presence of Acd and the aminoacyl-tRNA
599 synthetase/tRNA pair.
600

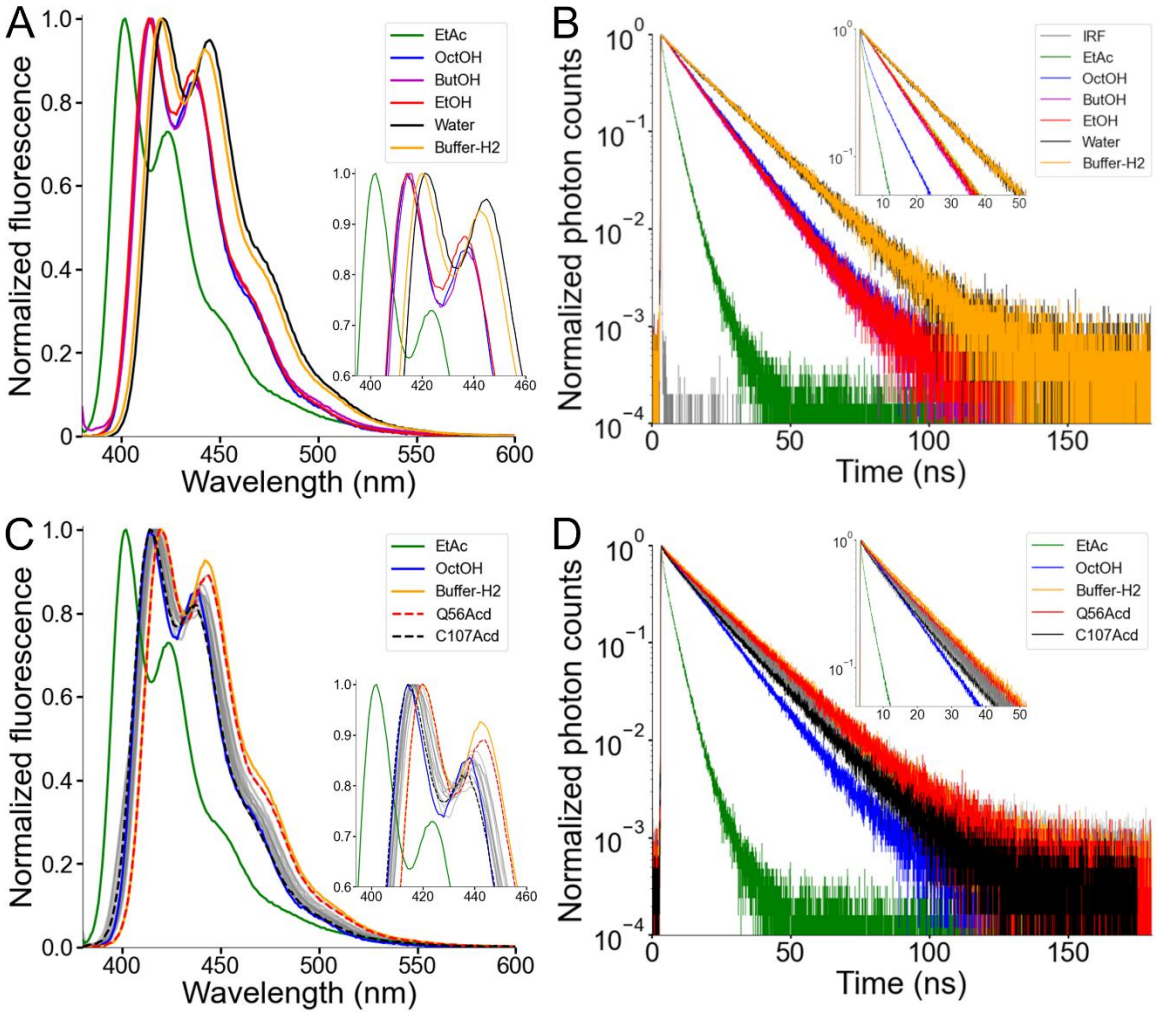

Figure 4. Acd showed a low environmental sensitivity in hH$_v$1. (A) Normalized fluorescence emission spectra of the Acd amino acid dissolved in the indicated solvent (Excitation = 370 nm). EtAc: ethyl acetate, OctOH: 1-octanol, ButOH: 1-butanol, EtOH: ethanol. (B) Normalized fluorescence decay of the Acd amino acid dissolved in the indicated solvent. (C) Normalized fluorescence emission spectra of the hH$_v$1-Acd proteins in Buffer-H2 (grey). The Acd amino acid spectra in selected solvents are also shown for reference. Q56Acd and C107Acd spectra are shown with broken lines. The emission maxima are listed in Table S3. (D) Normalized fluorescence decay of the hH$_v$1-Acd proteins in Buffer-H2 (grey). The Acd amino acid decays in selected solvents are also shown for reference. Q56Acd and C107Acd decays are shown in red and black, respectively.

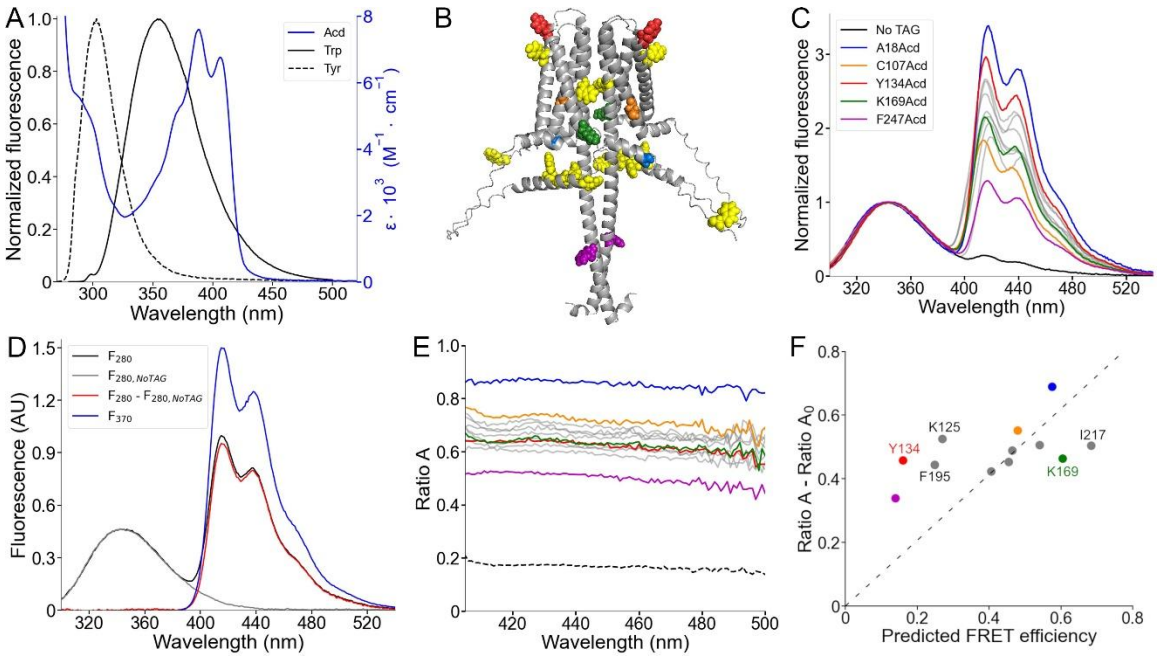

Figure 5. Spectral FRET analysis using Trp and Tyr donors and Acd as acceptor. (A) Fluorescence emission spectra of the intrinsic fluorescent amino acids Trp (black) and Tyr (black, broken lines), along with the Acd absorption spectrum in Buffer-H2 (blue). (B) AlphaFold dimer hH_v1 structural model with the amino acids colored according to (C) and the native tryptophan and tyrosine residues shown as yellow spheres. (C) Normalized fluorescence spectra of the purified hH_v1-Acd proteins (Excitation = 280 nm). The spectra were normalized by the Trp/Tyr fluorescence. The colors correspond to the indicated hH_v1-Acd protein, and the remaining spectra are shown as grey traces in the figure. The No TAG sample (black) contains purified hH_v1 protein without any amber stop codon expressed in the presence of Acd and the aminoacyl-tRNA synthetase/tRNA pair. (D) Example of the spectral FRET analysis procedure. The fluorescence spectrum of hH_v1-Y134Acd obtained when exciting at 280 nm (black, F_{280}) minus the normalized spectrum at the same excitation wavelength of the No TAG sample (grey, $F_{280,NoTAG}$) produced the Acd emission spectrum shown in red (F_{280} – $F_{280,NoTAG}$). *Ratio A* values were calculated by dividing this spectrum by the hH_v1-Y134Acd fluorescence spectrum obtained by direct excitation at 370 nm (F_{370}). (E) *Ratio A* traces of the hH_v1-Acd proteins colored according to (C). The ratio between the spectra of free Acd amino acid excited at 280 and 370 nm

635 (*Ratio* A_0) is shown as broken lines. (F) Mean *Ratio A* – *Ratio* A_0 values (410-480
636 nm; N=4) as a function of the predicted FRET efficiencies from the AlphaFold
637 hH_v1 structural model, colored according to (C). The broken line is the best fit to
638 the equation (*Ratio A* – *Ratio* A_0) = m(Predicted FRET efficiency).
639

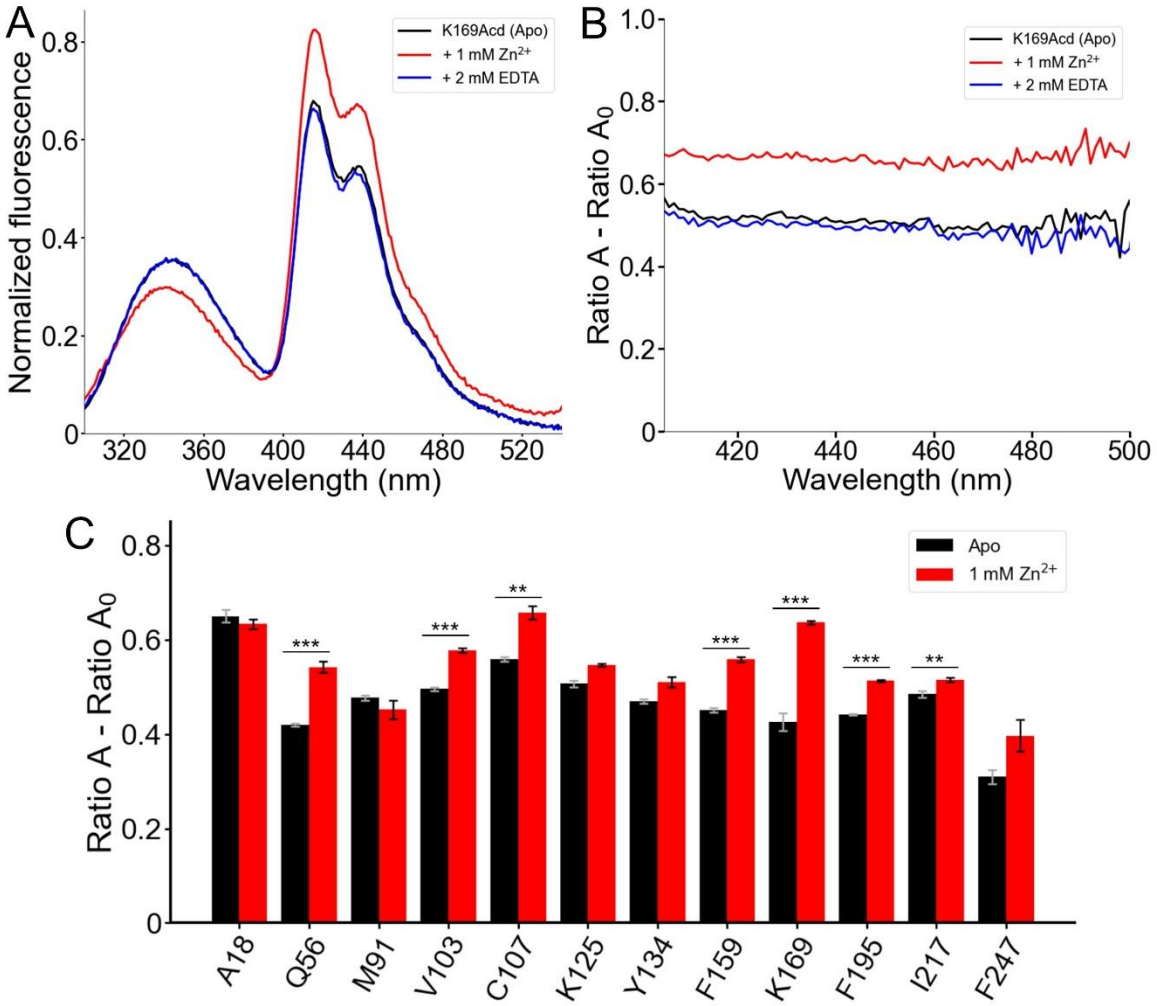

Figure 6. FRET between Trp/Tyr and Acd reports a conformational rearrangement in response to Zn^{2+}. (A) Normalized fluorescence emission spectra of hH_v1-K169Acd (Excitation = 280 nm) in Buffer-H2 in the absence of Zn^{2+} (black, Apo), in the presence of 1 mM Zn^{2+} (red), or in the presence of 1 mM Zn^{2+} and 2 mM EDTA (blue). Spectra were normalized by the maximum intensity of the Acd emission spectrum of the same sample excited at 370 nm. (B) Spectral FRET analysis of hH_v1-K169Acd in Buffer-H2 in the absence of Zn^{2+} (black, Apo), in the presence of 1 mM Zn^{2+} (red), or in the presence of 1 mM Zn^{2+} and 2 mM EDTA (blue). (C) Spectral FRET analysis of the hH_v1-Acd proteins in Buffer-H2 in the absence (black, Apo) or presence of 1 mM Zn^{2+} (red). N=4, ***$p<0.005$, **$p<0.01$.

Supplementary Text

Calculation of the FRET efficiency from the structural model. We calculated the FRET efficiency using the AlphaFold model of the full-length hH_v1 (Dataset S1). For each Acd position, the measured steady-state FRET would correspond to the mean FRET efficiency (E_{FRET}), which will be proportional to the *Ratio A – Ratio A_0* value obtained from the spectral FRET analysis.

For *n* number of donors and two acceptors in the hH_v1 dimer:

$$E_{FRET} = \sum_{i=1}^{n} P_{Ex,i} E_i \quad (1)$$

where $P_{Ex,i}$ is the probability of excitation and E_i is the FRET efficiency of the *i*th donor. $P_{Ex,i}$ is the number of photons absorbed by the *i*th donor divided by the total number of photons absorbed by the total number *n* of donors, which is quantified by the donor's extinction coefficient. Supposing the same extinction coefficient for each of the Trp (ε_W = 5,501 M^{-1} cm^{-1}) and Tyr (ε_Y = 1,209 M^{-1} cm^{-1}) (Supplementary Reference 1), equation 1 can be written as:

$$E_{FRET} = \sum_{i=1}^{n} \left(\frac{\varepsilon_i}{\sum_{i=1}^{n} \varepsilon_i}\right) E_i = \frac{1}{n_W \varepsilon_W + n_Y \varepsilon_Y} \left(\varepsilon_W \sum_{i=1}^{n_W} E_{W,i} + \varepsilon_Y \sum_{i=1}^{n_Y} E_{Y,i}\right) \quad (2)$$

where the sum of the total number of Trp (n_W) and Tyr (n_Y) is equal to *n*. The efficiency of FRET for the *i*th donor can be expressed as the sum of rates of energy transfer to each of the *j* = 2 Acd acceptors, k_{ij}, divided by the total rates of photon emission. Therefore, the right terms of equation 2 can be expressed as:

$$\sum_{i=1}^{n_W} E_{W,i} = \sum_{i=1}^{n_W} \left(\frac{\sum_{j=1}^{2} k_{ij}}{\sum_{j=1}^{2} k_{ij} + (1/\tau_W)}\right) \quad \text{and} \quad \sum_{i=1}^{n_Y} E_{Y,i} = \sum_{i=1}^{n_Y} \left(\frac{\sum_{j=1}^{2} k_{ij}}{\sum_{j=1}^{2} k_{ij} + (1/\tau_Y)}\right) \quad (3)$$

where the Trp lifetime (τ_W = 3.1 ns) and tyrosine lifetime (τ_Y = 3.6 ns) in the absence of donors are considered constant (Supplementary Reference 1). Finally, each energy transfer rate k_{ij} is a function of the distance r_{ij} between the *i*th donor and the *j*th acceptor:

$$k_{ij}(r) = \frac{1}{\tau_D} \left(\frac{R_0}{r_{ij}}\right)^6 \quad (4)$$

where the donor lifetime τ_D and R_0 would be τ_W and 23.5 Å or τ_Y and 20.9 Å for Trp or Tyr residues, respectively. For determining the R_0 values from the spectra overlap, we used an orientation factor value of 2/3, a refraction index of 1.3346 measured for BufferH2 using a refractometer, and quantum yields of 0.12 and

682 0.13 for Trp and Tyr, respectively (Supplementary Reference 1). Calculating
683 E_{FRET} using the above equations considers a fixed distance between donors and
684 acceptors. A better approach is to consider the distance distributions $P_{ij}(r)$
685 produced by the different rotameric states of the FRET pair, which can be
686 modeled easily using chiLife (Supplementary Reference 2). Then, equation 4 will
687 be replaced by equation 5:

688 $$k_{ij}(r) = \int_0^\infty P_{ij}(r) \left[\frac{1}{\tau_D}\left(\frac{R_0}{r}\right)^6\right] dr \quad (5).$$

689

690 **DNA plasmid sequences in FASTA format.**

691 >His-EK-hHv1-C107A-C249A.pET15-b

692 TTGAGATCCTTTTTTTCTGCGCGTAATCTGCTGCTTGCAAACAAAAAAACCAC
693 CGCTACCAGCGGTGGTTTGTTTGCCGGATCAAGAGCTACCAACTCTTTTTCC
694 GAAGGTAACTGGCTTCAGCAGAGCGCAGATACCAAATACTGTCCTTCTAGT
695 GTAGCCGTAGTTAGGCCACCACTTCAAGAACTCTGTAGCACCGCCTACATA
696 CCTCGCTCTGCTAATCCTGTTACCAGTGGCTGCTGCCAGTGGCGATAAGTC
697 GTGTCTTACCGGGTTGGACTCAAGACGATAGTTACCGGATAAGGCGCAGCG
698 GTCGGGCTGAACGGGGGGTTCGTGCACACAGCCCAGCTTGGAGCGAACGA
699 CCTACACCGAACTGAGATACCTACAGCGTGAGCTATGAGAAAGCGCCACGC
700 TTCCCGAAGGGAGAAAGGCGGACAGGTATCCGGTAAGCGGCAGGGTCGGA
701 ACAGGAGAGCGCACGAGGGAGCTTCCAGGGGGAAACGCCTGGTATCTTTA
702 TAGTCCTGTCGGGTTTCGCCACCTCTGACTTGAGCGTCGATTTTTGTGATGC
703 TCGTCAGGGGGGCGGAGCCTATGGAAAAACGCCAGCAACGCGGCCTTTTT
704 ACGGTTCCTGGCCTTTTGCTGGCCTTTTGCTCACATGTTCTTTCCTGCGTTA
705 TCCCCTGATTCTGTGGATAACCGTATTACCGCCTTTGAGTGAGCTGATACCG
706 CTCGCCGCAGCCGAACGACCGAGCGCAGCGAGTCAGTGAGCGAGGAAGC
707 GGAAGAGCGCCTGATGCGGTATTTTCTCCTTACGCATCTGTGCGGTATTTCA
708 CACCGCATATATGGTGCACTCTCAGTACAATCTGCTCTGATGCCGCATAGTT
709 AAGCCAGTATACACTCCGCTATCGCTACGTGACTGGGTCATGGCTGCGCCC
710 CGACACCCGCCAACACCCGCTGACGCGCCCTGACGGGCTTGTCTGCTCCC
711 GGCATCCGCTTACAGACAAGCTGTGACCGTCTCCGGGAGCTGCATGTGTCA

712 GAGGTTTTCACCGTCATCACCGAAACGCGCGAGGCAGCTGCGGTAAAGCT
713 CATCAGCGTGGTCGTGAAGCGATTCACAGATGTCTGCCTGTTCATCCGCGT
714 CCAGCTCGTTGAGTTTCTCCAGAAGCGTTAATGTCTGGCTTCTGATAAAGCG
715 GGCCATGTTAAGGGCGGTTTTTTCCTGTTTGGTCACTGATGCCTCCGTGTAA
716 GGGGGATTTCTGTTCATGGGGGTAATGATACCGATGAAACGAGAGAGGATG
717 CTCACGATACGGGTTACTGATGATGAACATGCCCGGTTACTGGAACGTTGT
718 GAGGGTAAACAACTGGCGGTATGGATGCGGCGGGACCAGAGAAAAATCAC
719 TCAGGGTCAATGCCAGCGCTTCGTTAATACAGATGTAGGTGTTCCACAGGG
720 TAGCCAGCAGCATCCTGCGATGCAGATCCGGAACATAATGGTGCAGGGCG
721 CTGACTTCCGCGTTTCCAGACTTTACGAAACACGGAAACCGAAGACCATTCA
722 TGTTGTTGCTCAGGTCGCAGACGTTTTGCAGCAGCAGTCGCTTCACGTTCG
723 CTCGCGTATCGGTGATTCATTCTGCTAACCAGTAAGGCAACCCCGCCAGCC
724 TAGCCGGGTCCTCAACGACAGGAGCACGATCATGCGCACCCGTGGCCAGG
725 ACCCAACGCTGCCCGAGATGCGCCGCGTGCGGCTGCTGGAGATGGCGGA
726 CGCGATGGATATGTTCTGCCAAGGGTTGGTTTGCGCATTCACAGTTCTCCG
727 CAAGAATTGATTGGCTCCAATTCTTGGAGTGGTGAATCCGTTAGCGAGGTG
728 CCGCCGGCTTCCATTCAGGTCGAGGTGGCCCGGCTCCATGCACCGCGACG
729 CAACGCGGGGAGGCAGACAAGGTATAGGGCGGCGCCTACAATCCATGCCA
730 ACCCGTTCCATGTGCTCGCCGAGGCGGCATAAATCGCCGTGACGATCAGC
731 GGTCCAGTGATCGAAGTTAGGCTGGTAAGAGCCGCGAGCGATCCTTGAAG
732 CTGTCCCTGATGGTCGTCATCTACCTGCCTGGACAGCATGGCCTGCAACGC
733 GGGCATCCCGATGCCGCCGGAAGCGAGAAGAATCATAATGGGGAAGGCCA
734 TCCAGCCTCGCGTCGCGAACGCCAGCAAGACGTAGCCCAGCGCGTCGGCC
735 GCCATGCCGGCGATAATGGCCTGCTTCTCGCCGAAACGTTTGGTGGCGGG
736 ACCAGTGACGAAGGCTTGAGCGAGGGCGTGCAAGATTCCGAATACCGCAA
737 GCGACAGGCCGATCATCGTCGCGCTCCAGCGAAAGCGGTCCTCGCCGAAA
738 ATGACCCAGAGCGCTGCCGGCACCTGTCCTACGAGTTGCATGATAAAGAAG
739 ACAGTCATAAGTGCGGCGACGATAGTCATGCCCCGCGCCCACCGGAAGGA
740 GCTGACTGGGTTGAAGGCTCTCAAGGGCATCGGTCGAGATCCCGGTGCCT
741 AATGAGTGAGCTAACTTACATTAATTGCGTTGCGCTCACTGCCCGCTTTCCA
742 GTCGGGAAACCTGTCGTGCCAGCTGCATTAATGAATCGGCCAACGCGCGG

743 GGAGAGGCGGTTTGCGTATTGGGCGCCAGGGTGGTTTTTCTTTTCACCAGT
744 GAGACGGGCAACAGCTGATTGCCCTTCACCGCCTGGCCCTGAGAGAGTTG
745 CAGCAAGCGGTCCACGCTGGTTTGCCCCAGCAGGCGAAAATCCTGTTTGAT
746 GGTGGTTAACGGCGGGATATAACATGAGCTGTCTTCGGTATCGTCGTATCC
747 CACTACCGAGATATCCGCACCAACGCGCAGCCCGGACTCGGTAATGGCGC
748 GCATTGCGCCCAGCGCCATCTGATCGTTGGCAACCAGCATCGCAGTGGGA
749 ACGATGCCCTCATTCAGCATTTGCATGGTTTGTTGAAAACCGGACATGGCAC
750 TCCAGTCGCCTTCCCGTTCCGCTATCGGCTGAATTTGATTGCGAGTGAGATA
751 TTTATGCCAGCCAGCCAGACGCAGACGCGCCGAGACAGAACTTAATGGGC
752 CCGCTAACAGCGCGATTTGCTGGTGACCCAATGCGACCAGATGCTCCACGC
753 CCAGTCGCGTACCGTCTTCATGGGAGAAAATAATACTGTTGATGGGTGTCT
754 GGTCAGAGACATCAAGAAATAACGCCGGAACATTAGTGCAGGCAGCTTCCA
755 CAGCAATGGCATCCTGGTCATCCAGCGGATAGTTAATGATCAGCCCACTGA
756 CGCGTTGCGCGAGAAGATTGTGCACCGCCGCTTTACAGGCTTCGACGCCG
757 CTTCGTTCTACCATCGACACCACCACGCTGGCACCCAGTTGATCGGCGCGA
758 GATTTAATCGCCGCGACAATTTGCGACGGCGCGTGCAGGGCCAGACTGGA
759 GGTGGCAACGCCAATCAGCAACGACTGTTTGCCCGCCAGTTGTTGTGCCAC
760 GCGGTTGGGAATGTAATTCAGCTCCGCCATCGCCGCTTCCACTTTTTCCCG
761 CGTTTTCGCAGAAACGTGGCTGGCCTGGTTCACCACGCGGGAAACGGTCT
762 GATAAGAGACACCGGCATACTCTGCGACATCGTATAACGTTACTGGTTTCAC
763 ATTCACCACCCTGAATTGACTCTCTTCCGGGCGCTATCATGCCATACCGCGA
764 AAGGTTTTGCGCCATTCGATGGTGTCCGGGATCTCGACGCTCTCCCTTATG
765 CGACTCCTGCATTAGGAAGCAGCCCAGTAGTAGGTTGAGGCCGTTGAGCAC
766 CGCCGCCGCAAGGAATGGTGCATGCAAGGAGATGGCGCCCAACAGTCCCC
767 CGGCCACGGGGCCTGCCACCATACCCACGCCGAAACAAGCGCTCATGAGC
768 CCGAAGTGGCGAGCCCGATCTTCCCCATCGGTGATGTCGGCGATATAGGC
769 GCCAGCAACCGCACCTGTGGCGCCGGTGATGCCGGCCACGATGCGTCCG
770 GCGTAGAGGATCGAGATCTCGATCCCGCGAAATTAATACGACTCACTATAG
771 GGGAATTGTGAGCGGATAACAATTCCCCTCTAGAAATAATTTTGTTTAACTTT
772 AAGAAGGAGATATACCATGGGCAGCAGCCATCATCATCATCATCACAGCAG
773 CGGCGATGATGATGATAAAATGGCGACCTGGGACGAAAAGGCGGTGACCC

774 GTCGTGCGAAAGTTGCGCCGGCGGAGCGTATGAGCAAGTTCCTGCGTCAC
775 TTTACCGTGGTTGGTGACGATTACCACGCGTGGAACATCAACTATAAGAAAT
776 GGGAGAACGAGGAAGAGGAAGAGGAAGAGGAACAGCCGCCGCCGACCCC
777 GGTTAGCGGCGAGGAAGGCCGTGCGGCGGCGCCGGATGTGGCGCCGGC
778 GCCGGGTCCGGCGCCGCGTGCGCCGCTGGATTTCCGTGGCATGCTGCGTA
779 AACTGTTCAGCAGCCACCGTTTTCAAGTTATCATTATCGCGCTGGTGGTTCT
780 GGATGCGCTGCTGGTGCTGGCGGAGCTGATCCTGGACCTGAAGATTATCCA
781 GCCGGATAAAAACAACTACGCGGCGATGGTTTTCCACTATATGAGCATCAC
782 CATTCTGGTGTTCTTTATGATGGAAATCATCTTCAAGCTGTTCGTTTTCCGTC
783 TGGAGTTCTTTCACCACAAATTCGAAATCCTGGACGCGGTGGTTGTGGTTGT
784 GAGCTTTATCCTGGATATTGTGCTGCTGTTCCAGGAGCACCAATTTGAAGCG
785 CTGGGTCTGCTGATTCTGCTGCGTCTGTGGCGTGTTGCGCGTATTATCAAC
786 GGCATTATCATTAGCGTGAAGACCCGTAGCGAGCGTCAGCTGCTGCGTCTG
787 AAGCAGATGAACGTTCAACTGGCGGCGAAAATCCAGCACCTGGAATTTAGC
788 GCGAGCGAGAAGGAACAAGAGATTGAACGTCTGAACAAACTGCTGCGTCAG
789 CACGGTCTGCTGGGCGAAGTGAACTAAGGATCCGGCTGCTAACAAAGCCC
790 GAAAGGAAGCTGAGTTGGCTGCTGCCACCGCTGAGCAATAACTAGCATAAC
791 CCCCTTGGGGCCTCTAAACGGGTCTTGAGGGGTTTTTTGCTGAAAGGAGGA
792 ACTATATCCGGATATCCCGCAAGAGGCCCGGCAGTACCGGCATAACCAAGC
793 CTATGCCTACAGCATCCAGGGTGACGGTGCCGAGGATGACGATGAGCGCA
794 TTGTTAGATTTCATACACGGTGCCTGACTGCGTTAGCAATTTAACTGTGATAA
795 ACTACCGCATTAAAGCTTATCGATGATAAGCTGTCAAACATGAGAATTCTTG
796 AAGACGAAAGGGCCTCGTGATACGCCTATTTTTATAGGTTAATGTCATGATA
797 ATAATGGTTTCTTAGACGTCAGGTGGCACTTTTCGGGGAAATGTGCGCGGA
798 ACCCCTATTTGTTTATTTTTCTAAATACATTCAAATATGTATCCGCTCATGAGA
799 CAATAACCCTGATAAATGCTTCAATAATATTGAAAAAGGAAGAGTATGAGTAT
800 TCAACATTTCCGTGTCGCCCTTATTCCCTTTTTTGCGGCATTTTGCCTTCCTG
801 TTTTTGCTCACCCAGAAACGCTGGTGAAAGTAAAAGATGCTGAAGATCAGTT
802 GGGTGCACGAGTGGGTTACATCGAACTGGATCTCAACAGCGGTAAGATCCT
803 TGAGAGTTTTCGCCCCGAAGAACGTTTTCCAATGATGAGCACTTTTAAAGTT
804 CTGCTATGTGGCGCGGTATTATCCCGTGTTGACGCCGGGCAAGAGCAACTC

GGTCGCCGCATACACTATTCTCAGAATGACTTGGTTGAGTACTCACCAGTCA
CAGAAAAGCATCTTACGGATGGCATGACAGTAAGAGAATTATGCAGTGCTG
CCATAACCATGAGTGATAACACTGCGGCCAACTTACTTCTGACAACGATCG
GAGGACCGAAGGAGCTAACCGCTTTTTTGCACAACATGGGGGATCATGTAA
CTCGCCTTGATCGTTGGGAACCGGAGCTGAATGAAGCCATACCAAACGACG
AGCGTGACACCACGATGCCTGCAGCAATGGCAACAACGTTGCGCAAACTAT
TAACTGGCGAACTACTTACTCTAGCTTCCCGGCAACAATTAATAGACTGGAT
GGAGGCGGATAAAGTTGCAGGACCACTTCTGCGCTCGGCCCTTCCGGCTG
GCTGGTTTATTGCTGATAAATCTGGAGCCGGTGAGCGTGGGTCTCGCGGTA
TCATTGCAGCACTGGGGCCAGATGGTAAGCCCTCCCGTATCGTAGTTATCT
ACACGACGGGGAGTCAGGCAACTATGGATGAACGAAATAGACAGATCGCTG
AGATAGGTGCCTCACTGATTAAGCATTGGTAACTGTCAGACCAAGTTTACTC
ATATATACTTTAGATTGATTTAAAACTTCATTTTTAATTTAAAAGGATCTAGGT
GAAGATCCTTTTTGATAATCTCATGACCAAAATCCCTTAACGTGAGTTTTCGT
TCCACTGAGCGTCAGACCCCGTAGAAAAGATCAAAGGATCTTC

>MjA9Acd-RS.pDule2
TTGAGATCGTTTTGGTCTGCGCGTAATCTCTTGCTCTGAAAACGAAAAAACC
GCCTTGCAGGGCGGTTTTTCGAAGGTTCTCTGAGCTACCAACTCTTTGAACC
GAGGTAACTGGCTTGGAGGAGCGCAGTCACCAAAACTTGTCCTTTCAGTTT
AGCCTTAACCGGCGCATGACTTCAAGACTAACTCCTCTAAATCAATTACCAG
TGGCTGCTGCCAGTGGTGCTTTTGCATGTCTTTCCGGGTTGGACTCAAGAC
GATAGTTACCGGATAAGGCGCAGCGGTCGGACTGAACGGGGGGTTCGTGC
ATACAGTCCAGCTTGGAGCGAACTGCCTACCCGGAACTGAGTGTCAGGCGT
GGAATGAGACAAACGCGGCCATAACAGCGGAATGACACCGGTAAACCGAA
AGGCAGGAACAGGAGAGCGCACGAGGGAGCCGCCAGGGGGAAACGCCTG
GTATCTTTATAGTCCTGTCGGGTTTCGCCACCACTGATTTGAGCGTCAGATT
TCGTGATGCTTGTCAGGGGGGCGGAGCCTATGGAAAAACGGCTTTGCCGC
GGCCCTCTCACTTCCCTGTTAAGTATCTTCCTGGCATCTTCCAGGAAATCTC
CGCCCCGTTCGTAAGCCATTTCCGCTCGCCGCAGTCGAACGACCGAGCGT
AGCGAGTCAGTGAGCGAGGAAGCGGAATATATCCTGTATCACATATTCTGC

836 TGACGCACCGGTGCAGCCTTTTTTCTCCTGCCACATGAAGCACTTCACTGAC
837 ACCCTCATCAGTGCCAACATAGTAAGCCAGTATACACTCCGCTAGCGCTGA
838 TGTCCGGCGGTGCTTTTGCCGTTACGCACCACCCCGTCAGTAGCTGAACAG
839 GAGGGACAGCTCCCGGCGGATTTGTCCTACTCAGGAGAGCGTTCACCGAC
840 AAACAACAGATAAAACGAAAGGCCCAGTCTTTCGACTGAGCCTTTCGTTTTA
841 TTTGATGCCTGGCAGTTCCCTACTCTCGCATGGGGAGACCCCACACTACCA
842 TCGGCGCTACGGCGTTTCACTTCTGAGTTCGGCATGGGGTCAGGTGGGAC
843 CACCGCGCTACTGCCGCCAGGCAAATTCTGTTTTATCAGACCGCTTCTGCG
844 TTCTGATTTAATCTGTATCAGGCTGAAAATCTTCTCTCATCCGCCAAAACAGC
845 CAAGCTGGAGACCGTTTAAACTCAATGATGATGATGATGATGGTCGACGGC
846 GCTATTCAGATCCTCTTCTGAGATGAGTTTTTGTTCGGGCCCAAGCTTCGAA
847 TTCCCATATGGTACCCGTTTGAAACTGCAGTTATAATCTCTTTCTAATTGGCT
848 CTAAAATCTTTATAAGTTCTTCAGCTACAGCATTTTTTAAATCCATTGGATGC
849 AATTCCTTATTTTTAAATAAACTCTCTAACTCCTCATAGCTATTAACTGTCAAA
850 TCTCCACCAAATTTTTCTGGCCTTTTTATGGTTAAAGGATATTCAAGGAAGTA
851 TTTAGCTATCTCCATTATTGGATTTCCTTCAACAACTCCAGCTGGGCAGTATG
852 CTTTCTTTATCTTAGCCCTAATCTCTTCTGGAGAGTCATCAACAGCTATAAAA
853 TTCCCTTTTGAAGAACTCATCTTTCCTTCTCCATCCAAACCCGTTAAGACAGG
854 GTTGTGAATACAAACAACCTTTTTTGGTAAAAGCTCCCTTGCTAACATGTTTA
855 TTTTTCTCTGCTCCATCCCTCCAACTGCAACATCAACGCCAGTATAATGAATA
856 GAATTAACCTGCATTATTGGATAGATAACTTCAGCAACCTTTGGATTTTCATC
857 CTCTCTTGCTATAAGTTCCATACTCCTTCTTGCTCTTTTTAAGGTAGTTTTTAA
858 AGCCAATCTATAGACATTCAGTGTATAATCCTTATCAAGCTCCAGTTCACTTC
859 CATAAACATATTTTGCCTTTAACCCCATTGCTTCAAAAACTTTTTTGTTATAAT
860 CTCCTATTTTTCTAATCTCATCCAACTCTCCTTTCTGGTTTAAATAGGCGTGT
861 AAATCAGCCAAATCTATAATTATATCAAATCCAGCATTTTGTAAATCAATCAT
862 CTTTTTTATTTGGAGATAATGCCCTAAATGTATTTTACCACTTGGTTCAAAAC
863 CTATCGCAGCAGATTTTTCATCTTTTTTTAAAACCTCTCTTAACTCTTCCTCG
864 CTGATAATTTCAGATGTGTTTCTCTTTATCATTTCAAATTCGTCCATGGGGGA
865 TTCCTCAAAGCGTAAACTCAGCGTTACAAGTATTACACAAAGTTTTTTATGTT
866 GAGAATATTTTTTTGATGGGGCGCCACTTATTTTTGATCGTTCGCTCAAAGAA

867 GCGGCGCCAGGGTTGTTTTTCTTTTCACCGGTGAGACGGGCAACAGAACGC
868 CATGAGCGGCCTCATTTCTTATTCTGAGTTACAACAGTCCGCACCGCTGTCC
869 GTATATATGAGTAAACTTGGTCCCGGGTTACCGGTTTGGTTAGCGAGAAGA
870 GCCAGTAAAAGACGCAGTGACGGCAATGTCTGATGCAATATGGACAATTGG
871 TTTCTTCTCTGAATGGCGGGAGTATGAAAAGTATGGCTGAAGCGCAAAATGA
872 TCCCCTGCTGCCGGGATACTCGTTTAATGCCCATCTGGTGGCGGGTTTAAC
873 GCCGATTGAGGCCAACGGTTATCTCGATTTTTTTATCGACCGACCGCTGGG
874 AATGAAAGGTTATATTCTCAATCTCACCATTCGCGGTCAGGGGGTGGTGAAA
875 AATCAGGGACGAGAATTTGTTTGCCGACCGGGTGATATTTTGCTGTTCCCG
876 CCAGGAGAGATTCATCACTACGGTCGTCATCCGGAGGCTCGCGAATGGTAT
877 CACCAGTGGGTTTACTTTCGTCCGCGCGCCTACTGGCATGAATGGCTTAAC
878 TGGCCGTCAATATTTGCCAATACGGGGTTCTTTCGCCCGGATGAAGCGCAC
879 CAGCCGCATTTCAGCGACCTGTTTGGGCAAATCATTAACGCCGGGCAAGGG
880 GAAGGGCGCTATTCGGAGCTGCTGGCGATAAATCTGCTTGAGCAATTGTTA
881 CTGCGGCGCATGGAAGCGATTAACGAGTCGCTCCATCCACCGATGGATAAT
882 CGGGTACGCGAGGCTTGTCAGTACATCAGCGATCACCTGGCAGACAGCAAT
883 TTTGATATCGCCAGCGTCGCACAGCATGTTTGCTTGTCGCCGTCGCGTCTG
884 TCACATCTTTTCCGCCAGCAGTTAGGGATTAGCGTCTTAAGCTGGCGCGAG
885 GACCAACGTATCAGCCAGGCGAAGCTGCTTTTGAGCACCACCCGGATGCCT
886 ATCGCCACCGTCGGTCGCAATGTTGGTTTTGACGATCAACTCTATTTCTCGC
887 GGGTATTTAAAAAATGCACCGGGGCCAGCCCGAGCGAGTTCCGTGCCGGT
888 TGTGAAGAAAAAGTGAATGATGTAGCCGTCAAGTTGTCATAATTGGTAACGA
889 ATCAGACAATTGACGGCTTGACGGAGTAGCATAGGGTTTGCAGAATCCCTG
890 CTTCGTCCATTTGACAGGCACATTATGCATGCCGCTTCGCCTTCGCGCGCG
891 AATTGATCTGCTGCCTCGCGCGTTTCGGTGATGACGGTGAAAACCTCTGAC
892 ACATGCAGCTCCCGGAGACGGTCACAGCTTGTCTGTAAGCGGATGCCGGG
893 AGCAGACAAGCCCGTCAGGGCGCGTCAGCGGGTGTTGGCGGGTGTCGGG
894 GCGCAGCCATGACCCAGTCAACTGCGATGAGTGGCAGGGCGGGGCGTAAT
895 TTTTTTAAGGCAGTTATTGGTGCCCTTAAACGCCTGGTTGCTACGCCTGAAT
896 AAGTGATAATAAGCGGATGAATGGCAGAAATTCGAAAGCAAATTCGACCCG
897 GTCGTCGGTTCAGGGCAGGGTCGTTAAATAGCCGCTTATGTCTATTGCTGG

898 TTTACCGGTTTATTGACTACCGGAAGCAGTGTGACCGTGTGCTTCTCAAATG
899 CCTGAGGCCAGTTTGCTCAGGCTCTCCCCGTGGAGGTAATAATTGACGATA
900 TGATCATTTATTCTGCCTCCCAGAGCATGATAAAAACGGTTAGCGCTTCGTT
901 AATACAGATGTAGGTGTTCCACAGGGTAGCCAGCAGCATCCTGCGATGCAG
902 ATCCGGAACATAATGGTGCAGGGCGCTTGTTTCGGCGTGGGTATGGTGGCA
903 GGCCCCGTGGCCGGGGGACTGTTGGGCGCTGCCGGCACCTGTCCTACGA
904 GTTGCATGATAAAGAAGACAGTCATAAGTGCGGCGACGATAGTCATGCCCC
905 GCGCCCACCGGAAGGAGCTACCGGCAGCGGTGCGGACTGTTGTAACTCAG
906 AATAAGAAATGAGGCCGCTCATGGCGTTCTGTTGCCCGTCTCACTGGTGAA
907 AAGAAAAACAACCCTGGCGCCGCTTCTTTGAGCGAACGATCAAAAATAAGT
908 GGCGCCCCATCAAAAAAATATTCTCAACATAAAAAACTTTGTGTAATACTTGT
909 AACGCTGAATTCCCGGCGGTAGTTCAGCAGGGCAGAACGGCGGACTCTAA
910 ATCCGCATGGCGCTGGTTCAAATCCGGCCCGCCGGACCACTGCAGATCCTT
911 AGCGAAAGCTAAGGATTTTTTTTAAGCTTGGCACTGGCCGTCGTTTTACAAC
912 GTCGTGACTGGGAAAACCCTGGCGTTACCCAACTTAATCGCCTTGCAGCAC
913 ATCCCCCTTTCGCCAGACGCTCTCCCTTATGCGACTCCTGCATTAGGAAGC
914 AGCCCAGTAGTAGGTTGAGGCCGTTGAGCACCGCCGCCGCAAGGAATGGT
915 GCATGCAAGGAGCCCGAGATGCGCCGCGTGCGGCTGCTGGAGATGGCGG
916 ACGCGATGGATATGTTCTGCCAAGGGTTGGTTTGCGCATTCACAGTTCTCC
917 GCAAGAATTGATTGGCTCCAATTCTTGGAGTGGTGAATCCGTTAGCGAGGT
918 GCCGCCGGCTTCCATTCAGGTCGAGGTGGCCCGGCTCCATGCACCGCGAC
919 GCAACGCGGGGAGGCAGACAAGGTATAGGGCGGCGCCTACAATCCATGCC
920 AACCCGTTCCATGTGCTCGCCGAGGCGGCATAAATCGCCGTGACGATCAG
921 CGGTCCAATGATCGAAGTTAGGCTGGTAAGAGCCGCGAGCGATCCTTGAAG
922 CTGTCCCTGATGGTCGTCATCTACCTGCCTGGACAGCATGGCCTGCAACGC
923 GGGCATCCCGATGCCGCCGGAAGCGAGAAGAATCATAATGGGGAAGGCCA
924 TCCAGCCTCGCGTCGCGAACGCCAGCAAGACGTAGCCCAGCGCGTCGGCC
925 GCCATGCCGGCGATAATGGCCTGCTTCTCGCCGAAACGTTTGGTGGCGGG
926 ACCAGTGACGAAGGCTTGAGCGAGGGCGTGCAAGATTCCGAATACCGCAA
927 GCGACAGGCCGATCATCGTCGCGCTCCAGCGAAAGCGGTCCTCGCCGAAA
928 ATGACCCAGAGCGCTGCCGGCACCTGTCCTACGAGTTGCATGATAAAGAAG

929 ACAGTCATAAGTGCGGCGACGATAGTCATGCCCCGCGCCCACCGGAAGGA
930 GCTGACTGGGTTGAAGGCTCTCAAGGGCATCGGTCGACGCTCTCCCTTATG
931 CGACTCCTGCATTAGGAAGCAGCCCAGTAGTAGGTTGAGGCCGTTGAGCAC
932 CGCCGCCGCAAGGAATGGTGCATGCAAGGAGATGGCGCCCAACAGTCCCC
933 CGGCCACGGGGCCTGCCACCATACCCACGCCGAAACAAGCGCTCATGAGC
934 CCGAAGTGGCGAGCCCGATCTTCCCCATCGGTGATGTCGGCGATATAGGC
935 GCCAGCAACCGCACCTGTGGCGCCGGTGATGCCGGCCACGATGCGTCCG
936 GCGTAGAGGATCCCGGTAAACCAGCAATAGACATAAGCGGCTATTTAACGA
937 CCCTGCCCTGAACCGACGACCGGGTCATCGTGGCCGGATCTTGCGGCCCC
938 TCGGCTTGAACGAATTGTTAGACATTATTTGCCGACTACCTTGGTGATCTCG
939 CCTTTCACGTAGTGGACAAATTCTTCCAACTGATCTGCGCGCGAGGCCAAG
940 CGATCTTCTTCTTGTCCAAGATAAGCCTGTCTAGCTTCAAGTATGACGGGCT
941 GATACTGGGCCGGCAGGCGCTCCATTGCCCAGTCGGCAGCGACATCCTTC
942 GGCGCGATTTTGCCGGTTACTGCGCTGTACCAAATGCGGGACAACGTAAGC
943 ACTACATTTCGCTCATCGCCAGCCCAGTCGGGCGGCGAGTTCCATAGCGTT
944 AAGGTTTCATTTAGCGCCTCAAATAGATCCTGTTCAGGAACCGGATCAAAGA
945 GTTCCTCCGCCGCTGGACCTACCAAGGCAACGCTATGTTCTCTTGCTTTTGT
946 CAGCAAGATAGCCAGATCAATGTCGATCGTGGCTGGCTCGAAGATACCTGC
947 AAGAATGTCATTGCGCTGCCATTCTCCAAATTGCAGTTCGCGCTTAGCTGGA
948 TAACGCCACGGAATGATGTCGTCGTGCACAACAATGGTGACTTCTACAGCG
949 CGGAGAATCTCGCTCTCTCCAGGGGAAGCCGAAGTTTCCAAAAGGTCGTTG
950 ATCAAAGCTCGCCGCGTTGTTTCATCAAGCCTTACGGTCACCGTAACCAGC
951 AAATCAATATCACTGTGTGGCTTCAGGCCGCCATCCACTGCGGAGCCGTAC
952 AAATGTACGGCCAGCAACGTCGGTTCGAGATGGCGCTCGATGACGCCAACT
953 ACCTCTGATAGTTGAGTCGATACTTCGGCGATCACCGCTTCCCTCATACTCT
954 TCCTTTTTCAATATTATTGAAGCATTTATCAGGGTTATTGTCTCATGAGCGGA
955 TACATATTTGAATGTATTTAGAAAAATAAACAAATAGCTAGCTCACTCGGTCG
956 CATCGATGATAAGCTGTCAAACATGAGAATTACAACTTATATCGTATGGGGC
957 TGACTTCAGGTGCTACATTTGAAGAGATAAATTGCACTGAAATCTAGAAATAT
958 TTTATCTGATTAATAAGATGATCTTC
959

960 **Supplementary Figures**

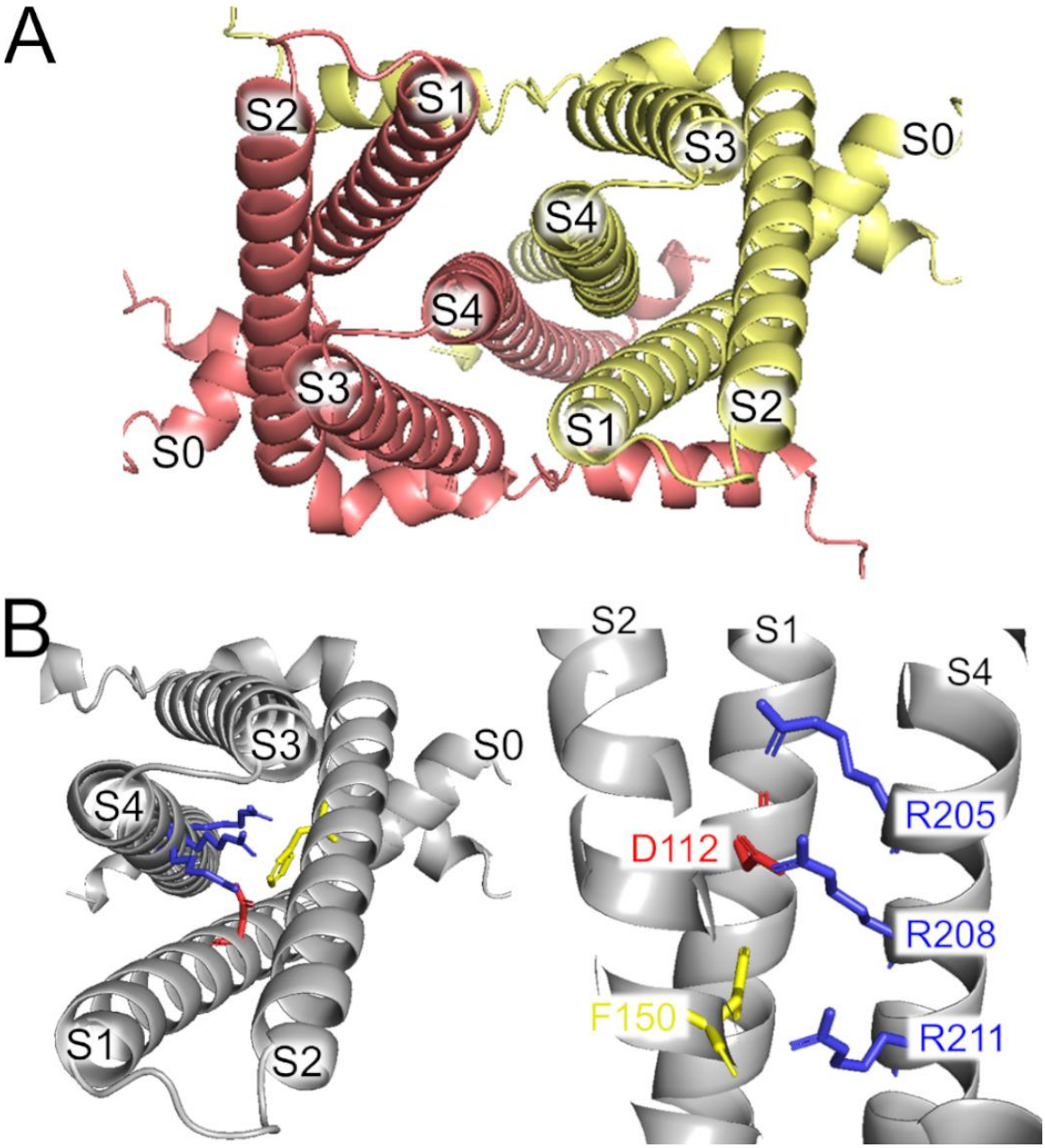

961

962 **Figure S1. AlphaFold dimer hH$_v$1 structural model.** (A) Extracellular view of
963 the model, showing each subunit in a different color. (B) One subunit of the dimer
964 showing the position of the arginine gating charges in S4 (blue), the selectivity
965 filter (red), and the charge transfer center (yellow).

966

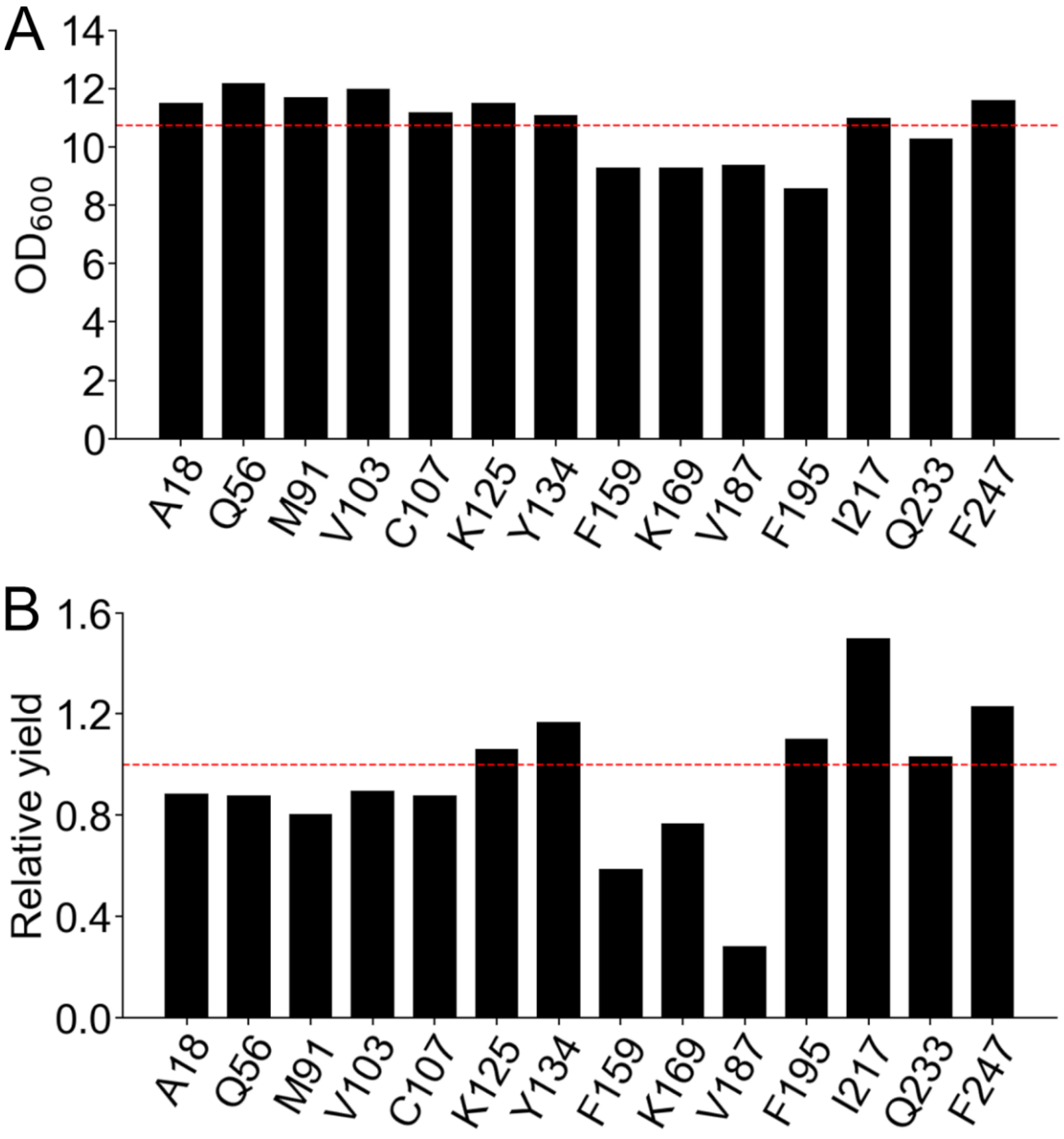

967

968 **Figure S2. The protein yield of hH$_v$1-Acd depended on the position of Acd**
969 **incorporation.** (A) Optical density at 600 nm (OD_{600}) of the final cultures
970 expressing the hH$_v$1 with Acd replacing the indicated amino acid. (B) Relative
971 protein yield calculated by multiplying the OD_{600} and Western blot band intensity
972 of cellular extracts from the final cultures expressing the hH$_v$1 with Acd replacing
973 the indicated amino acid. Values of normalized by the No TAG condition, which

974 are cells expressing the hH_v1 without any amber stop codon in the presence of
975 Acd and the aminoacyl-tRNA synthetase/tRNA pair (red broken line).
976

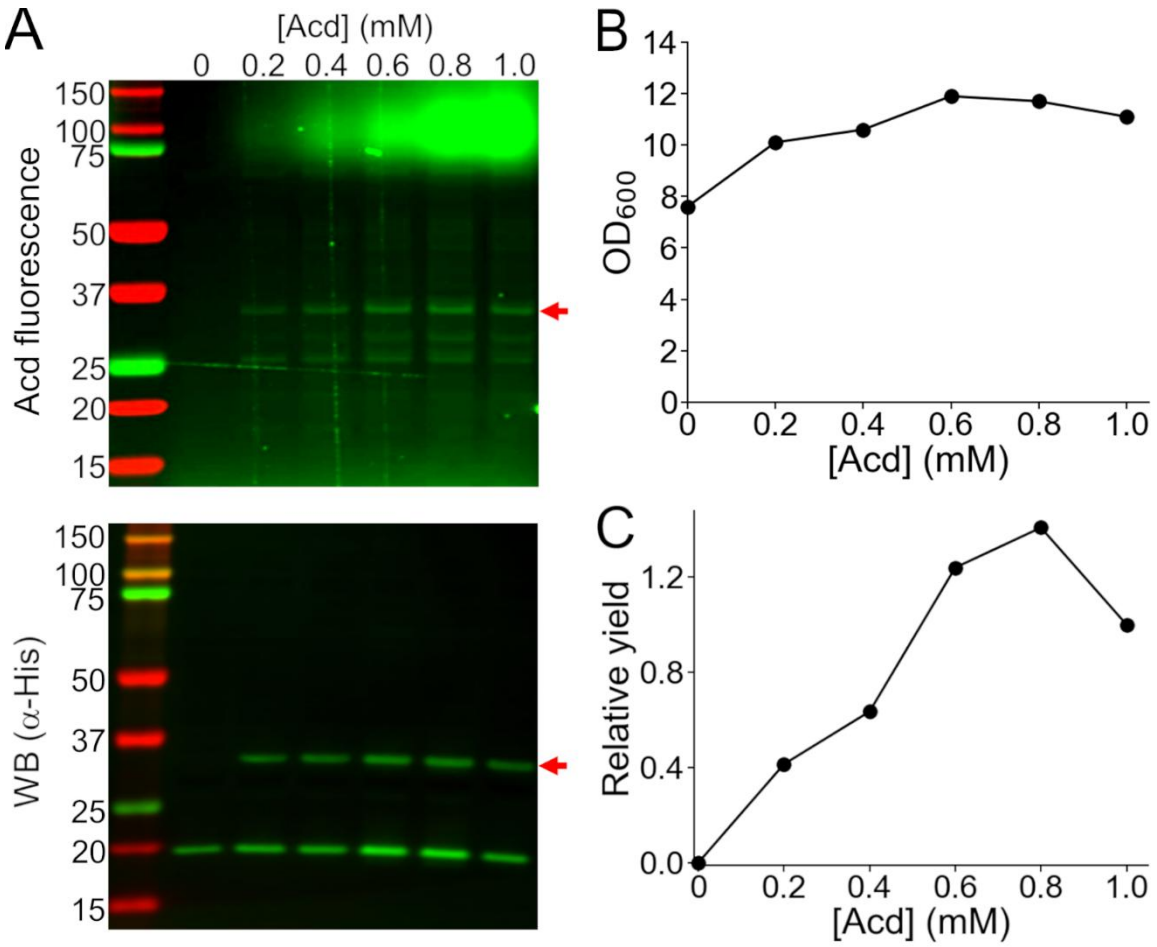

977

978

979 **Figure S3. The truncation of hH$_v$1-K125Acd was not decreased at higher**
980 **concentrations of Acd in the culture medium.** (A) Cellular extracts of cells co-
981 transformed with the MjA9-AcdRS/tRNA pair plasmid and hH$_v$1-K125TAG and
982 grown with the indicated concentration of Acd in the culture medium were
983 separated by SDS-PAGE to visualize the hH$_v$1 band (red arrow) by Acd
984 fluorescence (top) and Western blot against the N-terminus His-tag (bottom). (B)
985 Optical density at 600 nm (OD_{600}) of the cultures at the end of the expression. (C)

986 Relative yield obtained by multiplying the Western blot band intensity by the
987 OD600, normalized by the value obtained at 1 mM Acd.
988

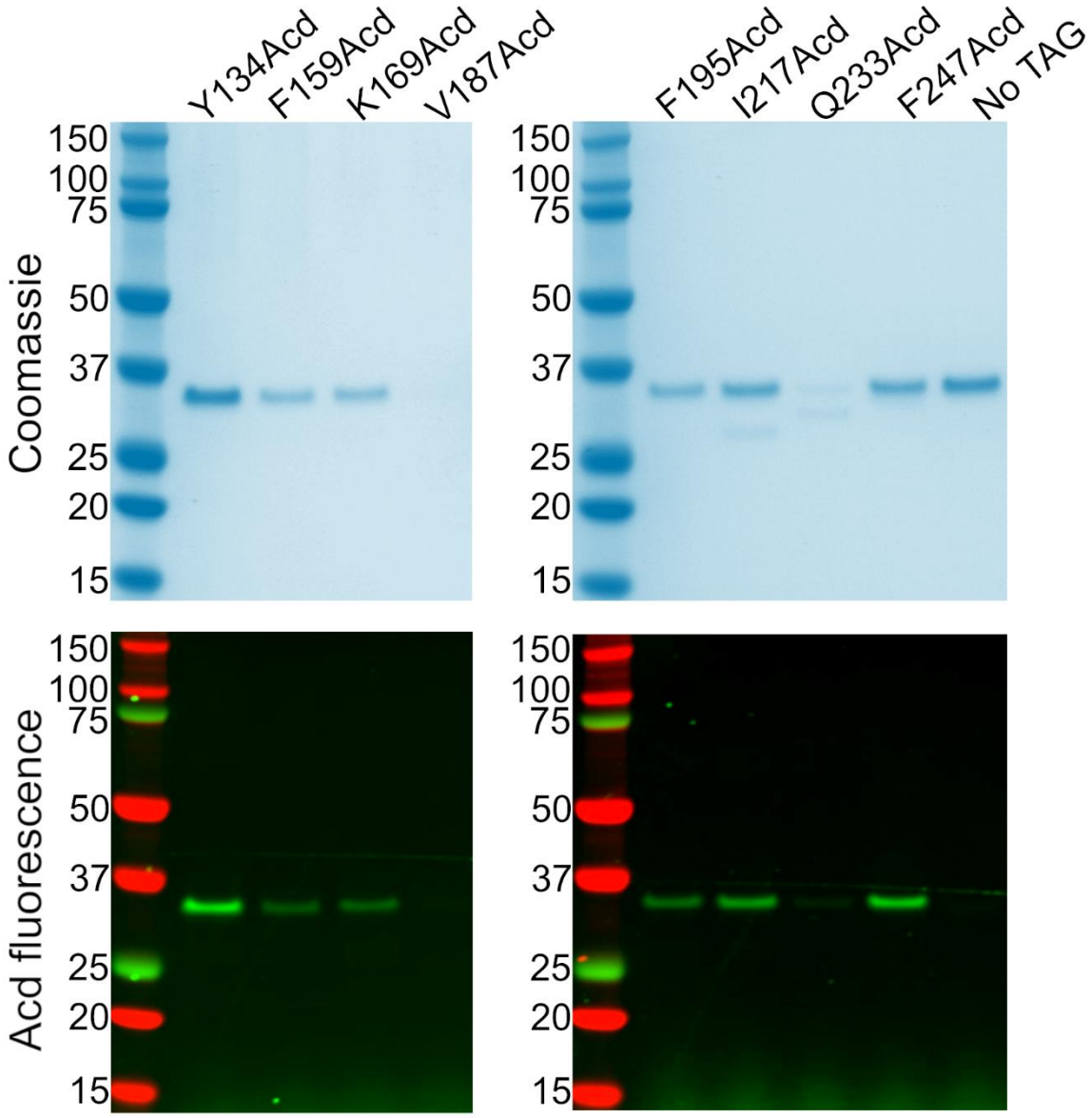

989

990 **Figure S4. SDS-PAGE of the hH$_v$1 protein samples after purification.**
991 Coomassie-stained (top) and Acd fluorescence (bottom) gels of the samples from
992 the elution of the nickel resin column, separated by SDS-PAGE. Note that
993 V187Acd and Q233Acd did not contain appreciable amounts of protein. The No
994 TAG condition consisted of samples purified from cells expressing the hH$_v$1
995 without any amber stop codon in the presence of Acd and the aminoacyl-tRNA
996 synthetase/tRNA pair.

997

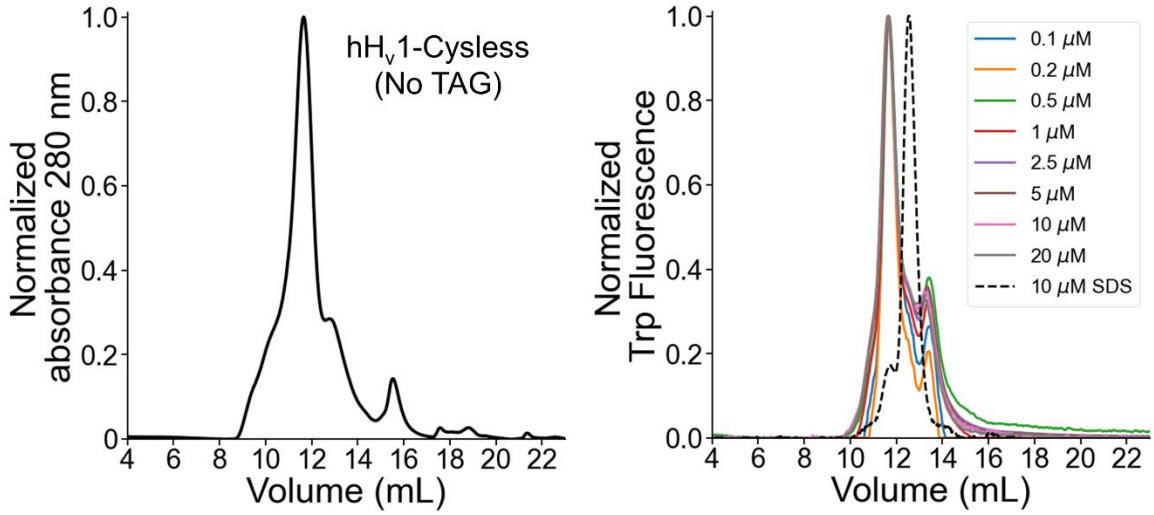

998

999 **Figure S5. The main hH$_v$1 peak in the size exclusion chromatogram**
1000 **corresponds to the dimer.** (Left) The No TAG sample was purified from cells
1001 expressing the hH$_v$1 without any amber stop codon in the presence of Acd and
1002 the aminoacyl-tRNA synthetase/tRNA pair. The sample eluted from the
1003 immobilized affinity chromatography column was concentrated and injected into
1004 the size exclusion chromatography column. (Right) SEC-cleaned samples were
1005 injected at the indicated concentration. The elution volumes of the samples were
1006 similar, with a mean ± standard deviation of 11.64 ± 0.01 mL. Additionally, a
1007 sample was run in a denaturing buffer containing 50 mM Tris, pH 8.0, 150 mM
1008 NaCl, and 0.2% SDS (dashed lines; elution volume of 12.5 mL). The invariant
1009 elution volume at low concentrations and higher elution volume in denaturing
1010 buffer strongly suggests that the main peak on the hH$_v$1 chromatograms
1011 corresponds to the dimer. The delay between the fluorescence and absorbance
1012 peaks is due to the physical separation of the detectors.

1013

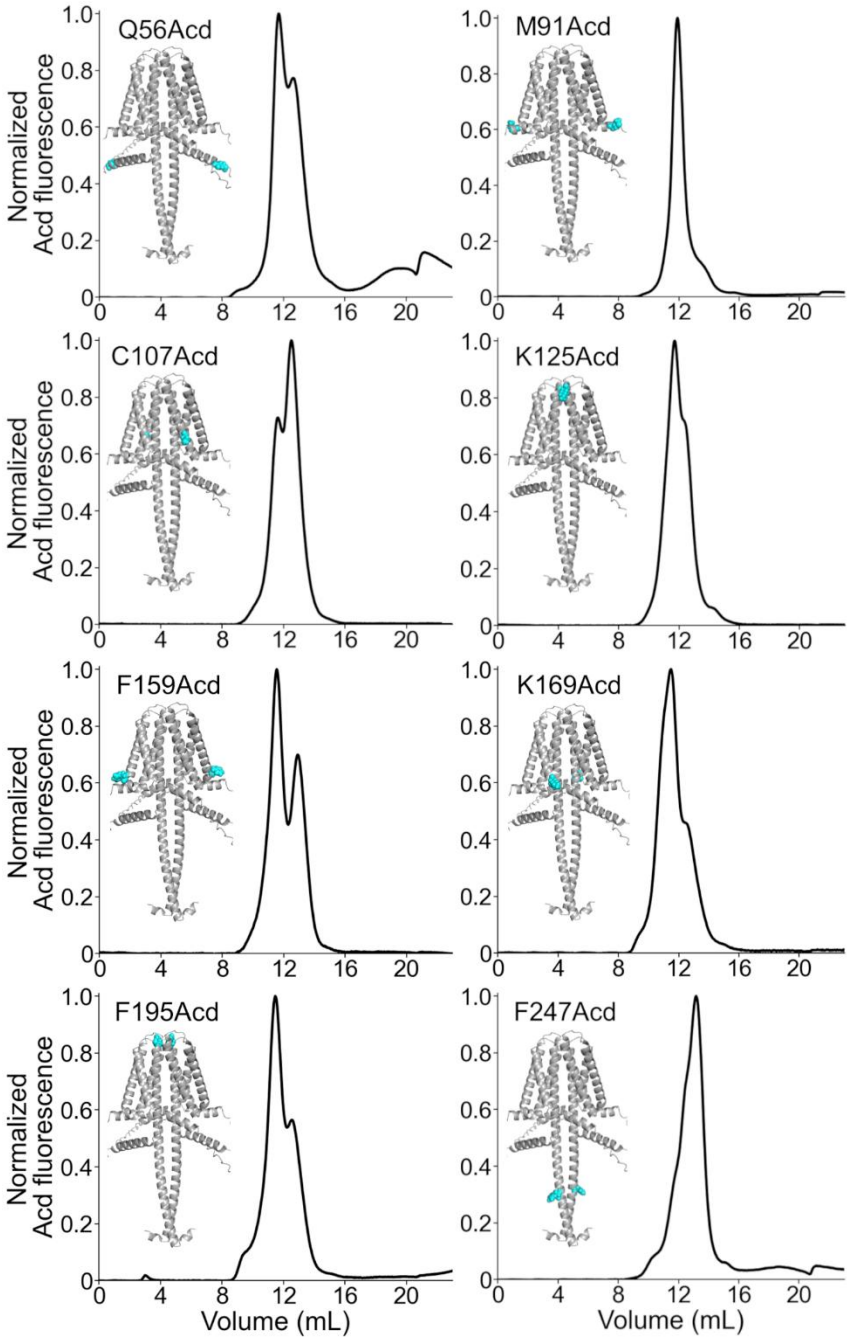

1014

1015 **Figure S6. Fluorescence-detection size exclusion chromatography of hH$_v$1-**
1016 **Acd proteins.** Chromatograms of the purified hH$_v$1 proteins with Acd
1017 incorporated at the indicated amino acid position. The AlphaFold dimer model
1018 with the amino acid replaced by Acd as cyan spheres is included.

1019

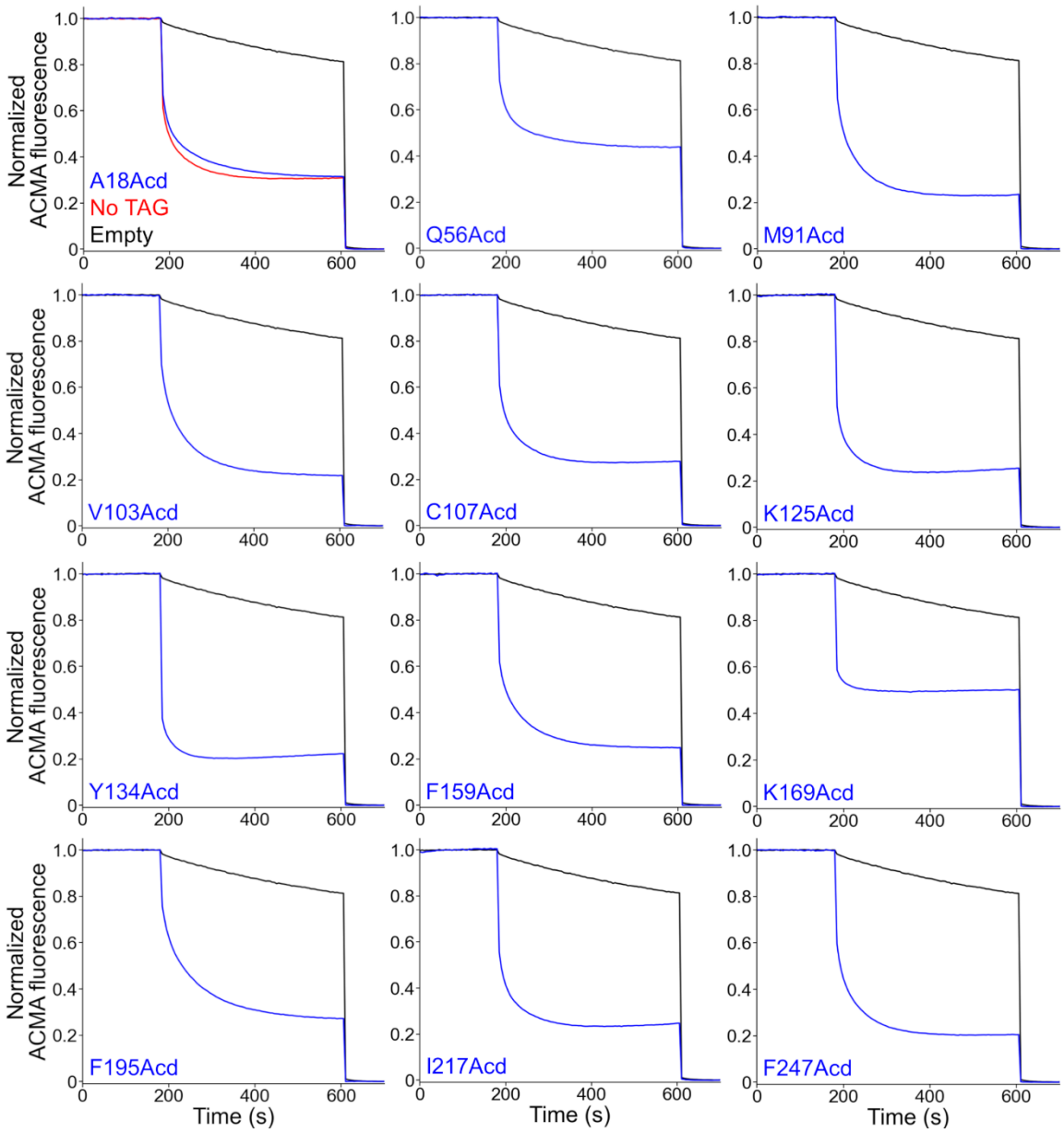

1020

1021 **Figure S7. The purified hH$_v$1-Acd proteins were functional proton channels.**
1022 Liposome proton flux assays of asolectin proteoliposomes containing the
1023 indicated hH$_v$1-Acd protein. The proteoliposome samples produced ACMA
1024 fluorescence quenching after the addition of valinomycin (180 s) in the presence
1025 of a potassium gradient. The protonophore CCCP was added at the end of the
1026 experiment (600 s). The No TAG sample (red trace) contains proteoliposomes
1027 containing hH$_v$1 without any amber stop codon expressed in the presence of Acd

1028 and the aminoacyl-tRNA synthetase/tRNA pair. Empty asolectin liposomes (black
1029 traces) showed slow ACMA fluorescence quenching.
1030

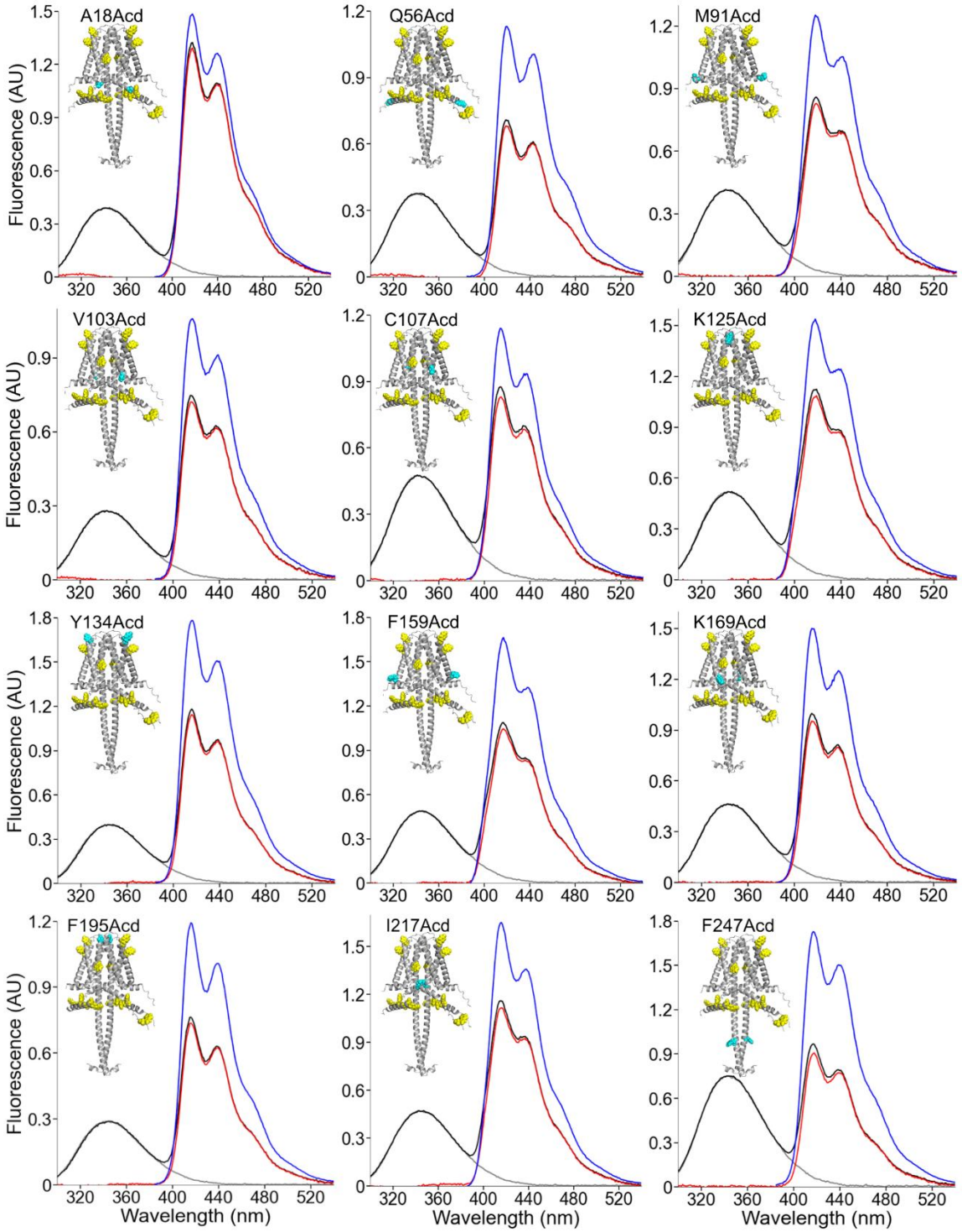

1031

1032 **Fig. S8. Fluorescence emission spectra of hH$_v$1-Acd.** Spectra of the indicated
1033 hH$_v$1-Acd protein sample obtained when exciting at 280 nm (black) and 370 nm
1034 (blue). The isolated spectrum of Acd (red) was obtained by subtracting the black

1035 trace from the normalized spectrum of the No TAG sample excited at 280 nm
1036 (grey).
1037

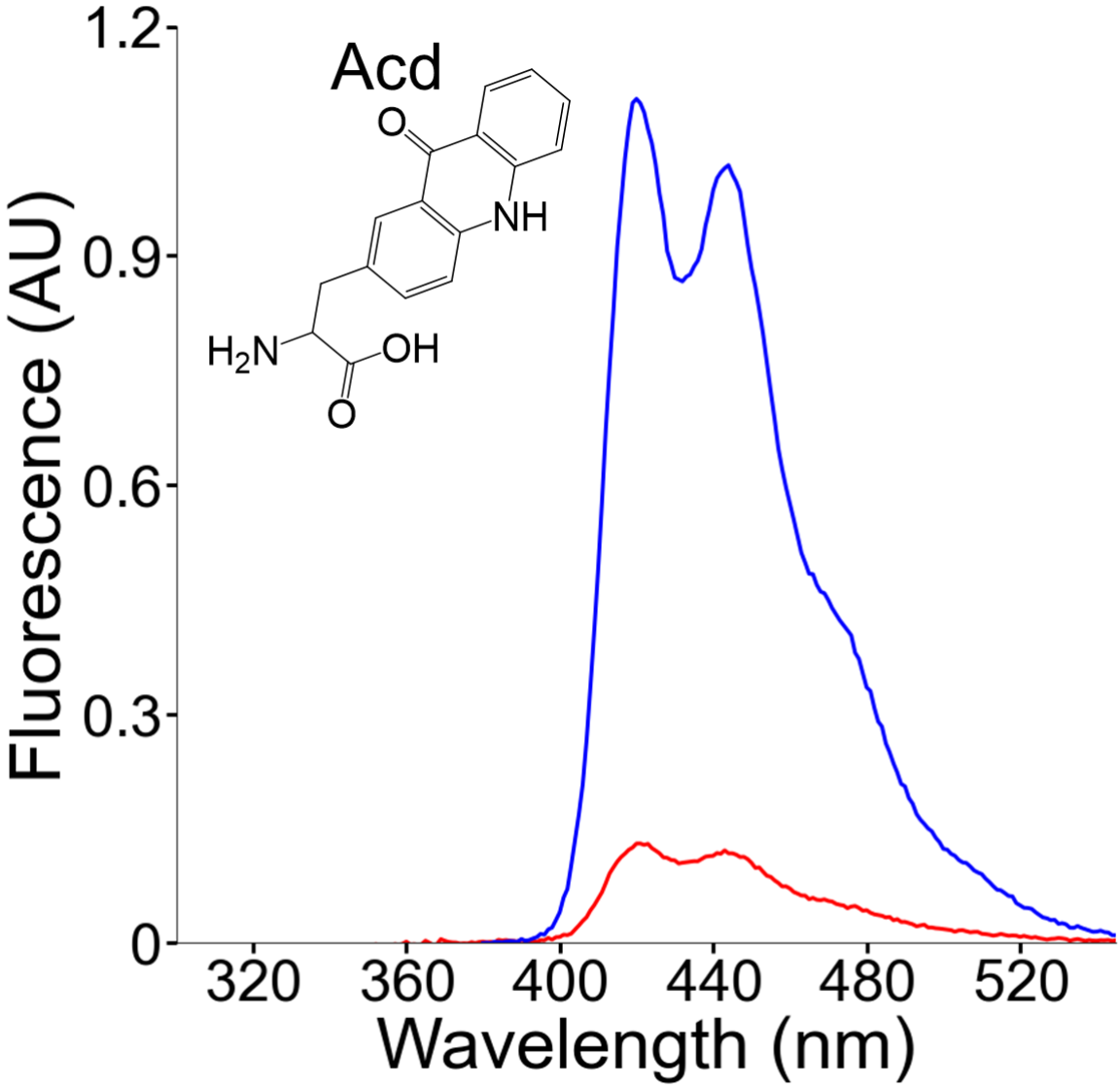

Figure S9. Fluorescence emission spectra of the Acd amino acid in solution. Spectra of Acd in Buffer-H2 using an excitation wavelength of 370 nm (blue) or 280 nm (red).

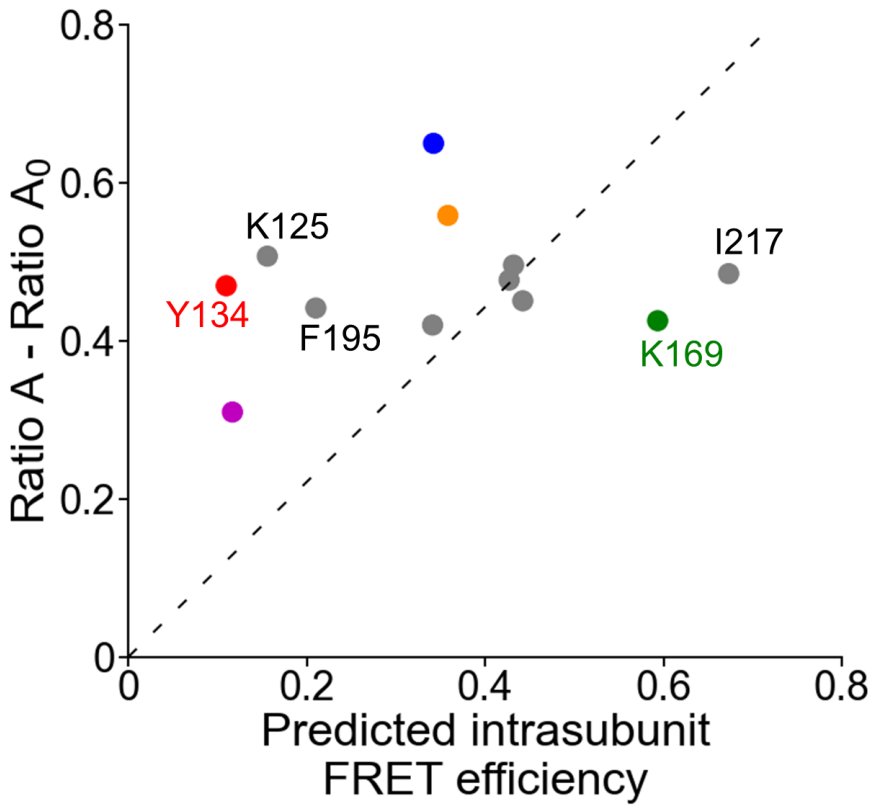

1043

1044 **Figure S10. Fluorescence emission spectra of the Acd amino acid in**
1045 **solution.** Mean *Ratio A – Ratio* A_0 values (410-480 nm; N=4) as a function of the
1046 predicted intrasubunit FRET efficiencies from one subunit of the AlphaFold hH_v1
1047 structural model, colored according to Figure 5F. The broken line is the best fit to
1048 the equation (*Ratio A – Ratio* A_0) = m(Predicted intrasubunit FRET efficiency).

1049

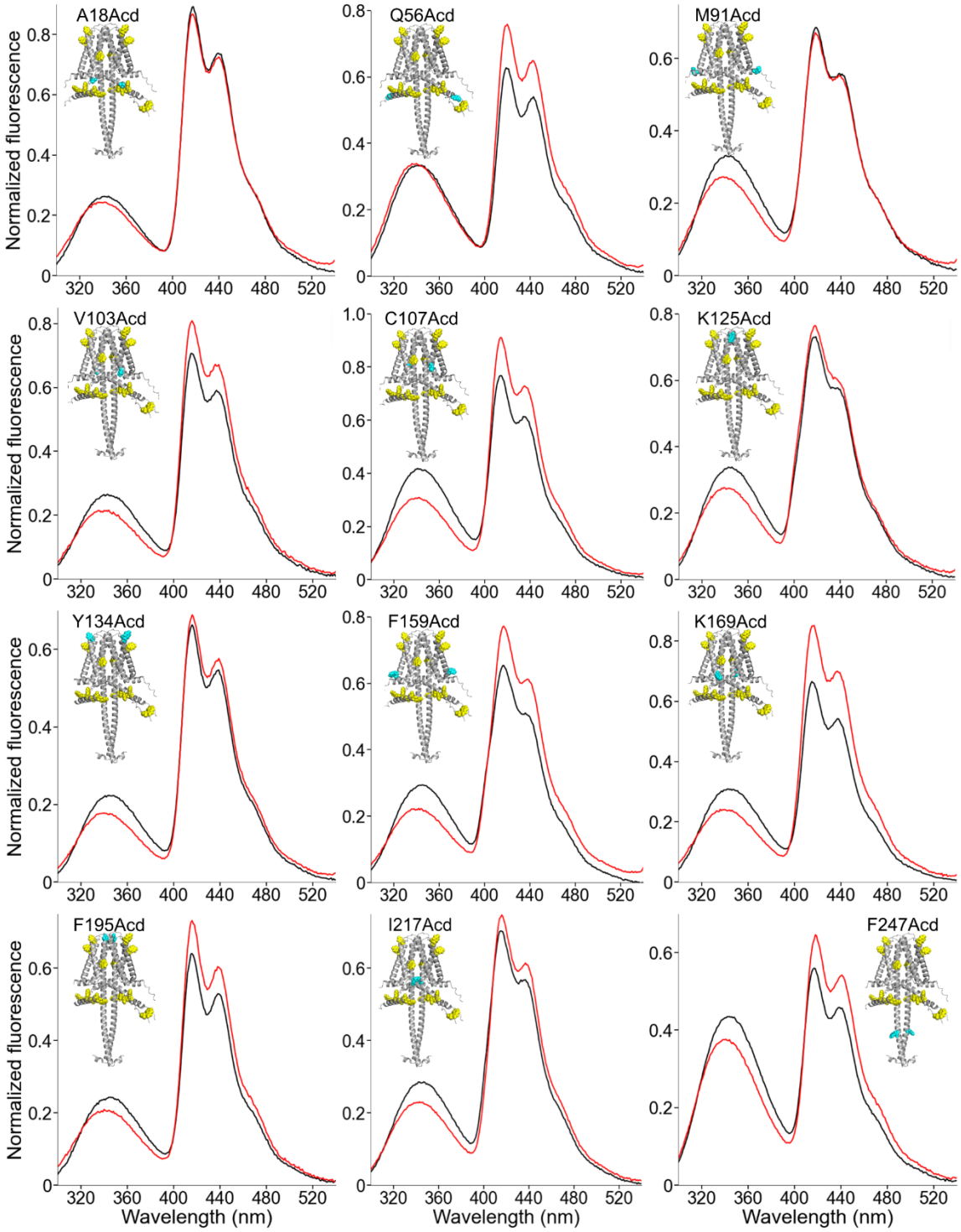

1050

1051 **Fig. S11. Changes in the fluorescence emission spectra of hH$_v$1-Acd in the**
1052 **presence of zinc.** Spectra of the indicated hH$_v$1-Acd protein sample obtained
1053 when exciting at 280 nm in the Apo state (black) and in the presence of 1 mM

1054 Zn^{2+} (red). Spectra were normalized by the maximum intensity of the Acd
1055 emission spectrum of the same sample excited at 370 nm.
1056

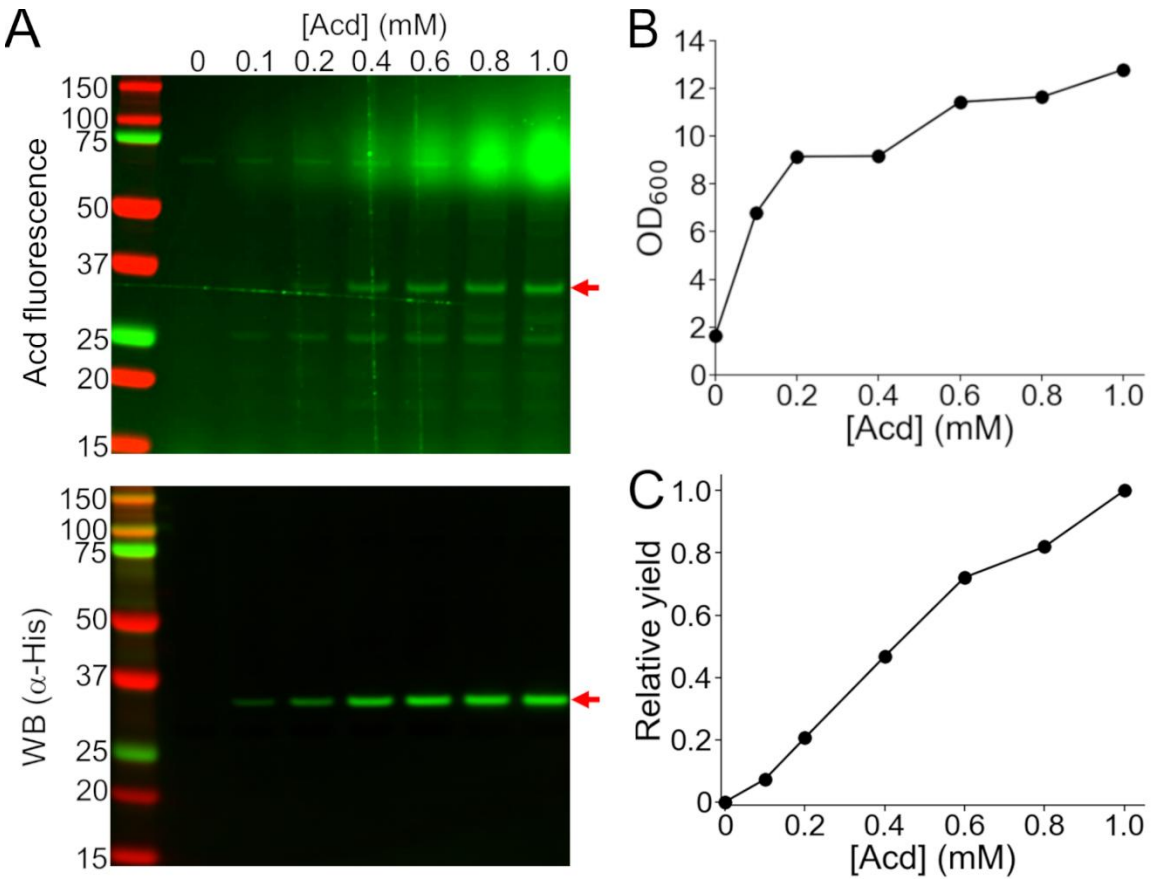

1057

1058 **Figure S12. The protein yield of hH$_v$1-A18Acd was proportional to the**
1059 **concentration of Acd in the culture medium.** (A) Cellular extracts of cells co-
1060 transformed with the MjA9-AcdRS/tRNA pair plasmid and hH$_v$1-A18TAG and
1061 grown with the indicated concentration of Acd in the culture medium were
1062 separated by SDS-PAGE to visualize the hH$_v$1 band (red arrow) by Acd
1063 fluorescence (top) and Western blot against the N-terminus His-tag (bottom). (B)
1064 Optical density at 600 nm (OD_{600}) of the cultures at the end of the expression. (C)
1065 Relative yield obtained by multiplying the Western blot band intensity by the
1066 OD_{600}, normalized by the value obtained at 1 mM Acd.

1067

1068 **Supplementary Tables**

1069 **Table S1. Size-exclusion chromatography elution volumes of the hH_v1**
1070 **proteins.** Elution volumes were measured as the location of the maximum value
1071 of absorbance at 280 nm in the chromatograms.

hH_v1 sample	Elution volume (mL)
No TAG	11.5
A18Acd	11.6
Q56Acd	11.7
M91Acd	11.9
V103Acd	11.5
C107Acd	12.5
K125Acd	11.7
Y134Acd	11.5
F159Acd	11.5
K169Acd	11.5
F195 Acd	11.5
I217Acd	12.4
F247Acd	13.1

1072

1073

1074 **Table S2. Emission fluorescence spectrum maximum of Acd in different**
1075 **solvents.** The wavelength corresponds to the location of the maximum intensity
1076 of the emission fluorescence spectrum of the free amino acid dissolved in the
1077 corresponding solvent. EtAc: ethyl acetate, OctOH: 1-octanol, ButOH: 1-butanol,
1078 EtOH: ethanol.

Solvent	Emission Maximum (nm)
EtAc	402
OctOH	414
ButOH	415
EtOH	414
Water	421
Buffer-H2	420

1079

1080

1081 **Table S3. The emission fluorescence spectrum maximum of the hH_v1-Acd**
1082 **proteins.** The wavelength corresponds to the location of the maximum intensity
1083 of the emission fluorescence spectrum of the samples.

hH_v1 sample	Emission Maximum (nm)
A18Acd	418
Q56Acd	420
M91Acd	419
V103Acd	417
C107Acd	415
K125Acd	418
Y134Acd	416
F159Acd	418
K169Acd	415
F195 Acd	416
I217Acd	415
F247Acd	418

1084
1085

1086 **Supplementary Dataset S1 (separate file).** Coordinates of the AlphaFold
1087 predicted model of the hH_v1 dimer (in PDB format).

1088

1089

1090 **Supplementary References**

1091 1. J. R. Lakowicz, Ed., *Principles of Fluorescence Spectroscopy* (Springer US, 2006).

1092 2. M. H. Tessmer, S. Stoll, chiLife: An open-source Python package for in silico spin
1093 labeling and integrative protein modeling. *PLoS Comput Biol* 19, e1010834 (2023).

1094